

# TuneNSearch: a hybrid transfer learning and local search approach for solving vehicle routing problems

Arthur Corrêa<sup>a</sup>, Cristóvão Silva<sup>a</sup>, Liming Xu<sup>b</sup>, Alexandra Brintrup<sup>b</sup>, Samuel Moniz<sup>a,\*</sup>

<sup>a</sup>*Department of Mechanical Engineering, CEMMPRE, ARISE, Universidade de Coimbra, Coimbra, Portugal*

<sup>b</sup>*Supply Chain AI Lab, Institute for Manufacturing, Department of Engineering, University of Cambridge, Cambridge, CB3 0FS, UK*

---

## Abstract

This paper introduces TuneNSearch, a hybrid transfer learning and local search approach for addressing different variants of the vehicle routing problem (VRP). Recently, multi-task learning has gained much attention for solving VRP variants. However, this adaptability often compromises the performance of the models. To address this challenge, we first pre-train a reinforcement learning model on the multi-depot VRP (MDVRP), followed by a fine-tuning phase to adapt it to different variants. In more detail, TuneNSearch employs, in the first stage, a Transformer-based architecture, augmented with a residual edge-graph attention network to capture the impact of edge distances and residual connections between layers. This architecture allows for a more precise capture of graph-structured data, improving the encoding of VRP’s features. After inference, our model is also coupled with a second stage composed of a local search algorithm, which yields substantial performance gains with small computational overhead added. Results show that TuneNSearch outperforms many existing state-of-the-art models trained for each VRP variant. The inherent complexity of the MDVRP enables the pre-trained model to generalize effectively to single-depot variants, achieving performance comparable to models trained specifically on single-depot instances. Moreover, it also demonstrates strong performance on multi-depot variants — a capability that models pre-trained exclusively on single-depot problems do not possess. Finally, through numerous experiments on randomly generated instances and benchmark public datasets, we show that our approach demonstrates strong generalization, achieving high performance across different tasks, distributions and problem sizes, thus addressing a long-standing gap in the literature.

**Keywords:** Vehicle Routing Problem, Combinatorial Optimization, Learning to Route, Local Search

---

## 1. Introduction

Vehicle routing problems (VRP) are a class of combinatorial optimization problems that hold particular importance in both academic literature and real-world settings. These problems are particularly relevant in fields such as city and food logistics, transportation and drone delivery (Cattaruzza et al., 2017; Li et al., 2019; Wang and Sheu, 2019; Wu et al., 2023). In short, they entail finding the most efficient route to visit a set of predefined nodes (such as delivery or service locations) using one or more vehicles, with the goal of minimizing the total traveled distance. Routing problems encompass numerous variants, including the traveling salesman problem (TSP), the capacitated vehicle routing problem (CVRP), the multi-depot vehicle routing problem (MDVRP), CVRP with backhauls, and other variants that introduce additional constraints (Elatar et al., 2023).

---

\*Corresponding author.

Email: samuel.moniz@dem.uc.pt

Address: Pólo II da Universidade de Coimbra, Rua Luís Reis Santos, 3030-788, Coimbra, Portugal

Phone: +351 239 790 712

The combinatorial characteristics of the VRP and its variants make these problems very difficult to solve optimally. Their inherent NP-hardness and intractability often render exact methods impractical, especially when solving large-scale problems with complicated constraints. Alternatively, meta-heuristics rely on search techniques to explore the solution space more efficiently. In this field, numerous methods have achieved notable performance on different routing problems, including LKH-3 (Helsgaun, 2017), hybrid genetic search (Vidal, 2022) and PyVRP (Wouda et al., 2024). However, despite presenting good results when solving complicated problems, compared with exact approaches, even the most efficient meta-heuristics still face significant computational burden as problem size grows. As a result, their applicability is limited in real-world cases, where rapid and precise decision-making is critical (Li et al., 2023).

In recent years, approaches based on neural networks have been gaining traction as an alternative to exact methods and meta-heuristics. These methods use neural networks to learn policies that can approximate good quality solutions with minimal computational overhead and little domain-specific knowledge. Most neural-based methods are trained using supervised or reinforcement learning algorithms and can be divided into two categories: construction and improvement approaches. The former is more predominant and refers to algorithms that can generate solutions in an end-to-end fashion, such as Kool et al. (2019), Kwon et al. (2020) and Zhou et al. (2023). The latter methods have the capability to learn policies that iteratively improve an initially generated solution (Hudson et al., 2022; Roberto et al., 2020; Wu et al., 2022; Xin et al., 2021).

While neural-based methods demonstrate promising results, they are often tailored for specific types of routing problems, similar to meta-heuristics, which are typically designed for particular cases. This specialization limits their ability to generalize across different problem variants. Recent research efforts have sought to address this challenge. For instance, Liu et al. (2024) proposed a multi-task learning method that utilizes attribute composition to solve different VRP variants. Meanwhile, Zhou et al. (2024a), explored a different approach, using a mixture-of-experts model to enhance cross-problem generalization. Although these studies offer valuable insights, they still fall short in matching the performance of neural-based models that are specifically trained for each VRP variant. Their improved adaptability is noteworthy, however, it comes at the expense of solution quality, making them less effective than specialized models. In contrast, Lin et al. (2024) explored a fine-tuning approach that adapts a backbone model, pre-trained on a standard TSP, to effectively solve other variants. While this method outperforms models trained independently for each variant, it requires a similar computational effort and a comparable number of training epochs in the fine-tuning phase, making it overall less computationally efficient.

From a practical perspective, the ability to develop a model that can generalize across different problems has profound implications, particularly in the most challenging manufacturing settings. As the demand for highly adaptable decision-support frameworks increases, practitioners are looking for solutions that can be customized to meet their specific needs (Jan et al., 2023). By reducing the reliance on multiple specialized models, businesses can conserve resources (both computational and manpower resources) and minimize the time required to develop and deploy solutions across different scenarios. This versatility could offer significant operational advantages, enabling companies to adapt more easily to changing routing conditions or new problem variants. However, as evidenced by the trade-offs in existing methods, achieving a balance between computational efficiency and solution quality remains a crucial challenge.

Motivated by this challenge, we introduce TuneNSearch, a novel fine-tuning transfer learning approach designed to tackle various routing problems. Transfer learning is a machine learning technique that allows a model trained on one task to be adapted for a different but related task (Pan and Yang, 2010). In this way, previously acquired knowledge can be leveraged to improve the learning performance and reduce training time. Specifically, we propose pre-training a model on the MDVRP, a variant that has been largely overlooked by existing neural-based methods. Through exploiting the complexity inherent to the MDVRP, our goal is for the pre-trained model to not only generalize effectively to single-depot variants, but also multi-depot scenarios — a capability that models pre-trained exclusively on single-depot problems lack. Given that existing neural-based methods often struggle with generalization, particularly for larger instances, our approach features a hybridization combining machine learning with a high-performance local search algorithm. Therefore, a two-stage process is proposed, where an efficient local search refines solutions after the initial inference stage. As a result, TuneNSearch achieves significant improvements in generalization,

substantially reducing the performance gaps compared to existing methods, such as [Kwon et al. \(2020\)](#), [Li et al. \(2024\)](#) and [Zhou et al. \(2024a\)](#). The key contributions of this work include:

- Development of a novel transfer learning method that is based on pre-training on the MDVRP, designed to adapt effectively to various VRP variants. Unlike simpler variants, the MDVRP incorporates a multi-depot structure in which vehicles can depart from multiple locations, thereby allowing the model to capture richer and more complex representations. Computational results show that this approach facilitates a more efficient generalization to solve both single- and multi-depot VRP variants.
- Proposal of a novel learning framework for solving the MDVRP. Our method employs a Transformer architecture ([Vaswani et al., 2017](#)) using the policy optimization with multiple optima (POMO) approach from [Kwon et al. \(2020\)](#). The proposed framework also integrates a residual edge-graph attention network (E-GAT), similar to [Lei et al. \(2022\)](#), to capture the impact of edge information and residual connections between consecutive layers. Unlike [Lei et al. \(2022\)](#), who applied the residual E-GAT encoder to the attention model from [Kool et al. \(2019\)](#), we extend it to POMO and the MDVRP. This extension enables a more accurate calculation of attention coefficients by incorporating edge distances during the feature encoding process. Our model outperforms the multi-depot multi-type attention (MD-MTA) approach proposed by [Li et al. \(2024\)](#). Specifically, in instances with 50 nodes, we reduced the performance gap by a factor of 6, and on instances with 100 nodes, by a factor of more than 2.
- Improvement of the inference process by integrating an efficient local search method. This local search algorithm employs a set of different operators to improve the solutions obtained by the E-GAT model, resulting in significant performance gains with small additional computational cost. As a result, the proposed method achieves new state-of-the-art performance among neural-based approaches. On 100-node instances, it obtains an average gap of less than 4% across all VRP variants compared to PyVRP ([Wouda et al., 2024](#)), while requiring only a fraction of the computational time.
- To verify the effectiveness of TuneNSearch, we solve numerous large-scale instances from CVRPLIB and TSPLIB. TuneNSearch demonstrates robust cross-distribution, cross-size and cross-task generalization, consistently exceeding other neural-based state-of-the-art methods in nearly all tested instances.

The rest of this paper is organized as follows. Section 2 discusses the relevant literature. Section 3 provides important preliminaries for this work. Section 4 elaborates on the model architecture, including the encoder, decoder, fine-tuning process and local search mechanism. Section 5 displays the computational experiments performed. Finally, Section 6 draws conclusions and limitations, and envisions possible future work.

## 2. Related work

This section briefly reviews three main research areas pertinent to this study. First, it examines optimization approaches for solving VRPs, including exact methods and meta-heuristics. Second, it discusses the most relevant neural-based methods developed in this field. Third, it explores multi-task learning and transfer learning techniques, which is an emerging field dedicated to creating models that can effectively address various VRP variants.

### 2.1. Solving VRPs with exact methods and meta-heuristics

Over the last few decades, a variety of methods have been proposed to address routing problems, including exact methods and meta-heuristic algorithms. Exact methods are fundamentally limited in their ability to guarantee optimal solutions within polynomial time. As a result, their application is typically limited to small- and medium-sized problem instances. The development and application of exact methods for routing problems has been reviewed by [Baldacci et al. \(2012\)](#) and [Zhang et al. \(2022\)](#). Most of these methods involve techniques such as branch-and-cut, dynamic programming and set partitioning formulations. More

recently, [Pessoa et al. \(2020\)](#) introduced a generic solver based on a branch-cut-and-price algorithm capable of solving different routing problem variants. Nevertheless, the method remains computationally intractable for instances involving more than a few hundred nodes.

Alternatively, meta-heuristic algorithms are far more prevalent than exact methods in the literature ([Braekers et al., 2016](#)). Unlike exact approaches, meta-heuristics do not guarantee optimal solutions, as a complete search of the solution space cannot be proven. However, these methods tend to be more efficient, utilizing advanced exploration techniques to find high-quality solutions — often reaching optimal solutions — in significantly less time. The first meta-heuristic method for the MDVRP was proposed by [Renaud et al. \(1996\)](#), introducing a tabu search algorithm that constructs an initial solution by assigning each customer to its nearest depot. The approach consists of three phases: fast-improvement, intensification and diversification. [Marinakis and Marinaki \(2010\)](#) combined a genetic algorithm with particle swarm optimization for the CVRP, allowing individual solutions within the population to evolve throughout their lifetime. This approach reduced computational time and improved scalability to larger problem instances compared to other meta-heuristics. [Helsgaun \(2017\)](#) introduced LKH-3, a heuristic method capable of solving various routing problem variants. It transforms the problems into a constrained TSP and utilizes the LKH local search ([Helsgaun, 2000](#)) to effectively explore the solution space. [Silva et al. \(2019\)](#) designed a multi-agent meta-heuristic framework combined with reinforcement learning for solving the VRP with time windows. In this framework, each meta-heuristic is represented as an autonomous agent that collaborates with others, enhancing solution quality through cooperative behavior. [Vidal \(2022\)](#) presented a hybrid genetic search for the CVRP and introduced the new *Swap\** operator. Rather than swapping two customers directly in place, this operator proposes exchanging two customers from different routes by inserting them into any position on the opposite route. This work has become a standard in CVRP literature, achieving state-of-the-art performance across various benchmarks. [Kalatzantonakis et al. \(2023\)](#) presented a hybrid approach between reinforcement learning and a variable neighborhood search for the CVRP, utilizing different upper confidence bound algorithms for adaptive neighborhood selection. More recently, [Wouda et al. \(2024\)](#) introduced PyVRP, an open-source VRP solver package. PyVRP offers a high-performance implementation of the hybrid genetic search algorithm ([Vidal, 2022](#)) and supports extensive customization options, making it suitable for a variety of VRP variants. Lastly, OR-Tools ([Furnon and Perron, 2024](#)) is a general-purpose optimization toolkit designed to solve a wide range of combinatorial problems. It includes a robust routing library capable of addressing various VRP variants, offering greater versatility than the previously cited works. OR-Tools uses a first-solution heuristic to generate an initial solution, followed by a guided local search to iteratively improve it. Subsequently, it employs a constraint programming approach to check whether the solution satisfies all specified constraints.

## 2.2. Neural-based combinatorial optimization for VRPs

Although meta-heuristics are generally more computationally efficient than exact methods, their execution time still increases significantly with the instance size. In this sense, neural-based methods surged in recent years as an alternative to solve combinatorial problems ([Bengio et al., 2021](#); [Mazyavkina et al., 2021](#)). By recognizing patterns in data, these methods can learn policies, obtaining high-quality solutions in polynomial time, even for large and hard to solve instances.

Currently, there exists two main categories of neural methods for solving routing problems: construction-based and improvement-based methods. Construction-based methods learn a policy to construct solutions incrementally, starting from an empty set and building routes step by step in an autoregressive manner. [Vinyals et al. \(2015\)](#) introduced Pointer Networks, a sequence-to-sequence model that addressed the problem of variable-sized outputs by using a ‘pointer’ mechanism to select elements from the input sequence as the output. Their approach was applied to solve the TSP and trained using supervised learning, being an early demonstration of the potential of neural networks for combinatorial optimization. Later, [Bello et al. \(2017\)](#) built on this approach by using a similar model architecture but training it with reinforcement learning. This eliminated the need for (near)-optimal labels and led to improved performance over Pointer Networks. [Nazari et al. \(2018\)](#) extended the architecture of Pointer Networks to handle dynamic elements in problems. Their approach proved effective in solving more challenging combinatorial problems, such as the stochastic VRP and VRP with split deliveries. [Kool et al. \(2019\)](#) made a significant contribution to

recent literature by proposing an attention model that utilizes a Transformer architecture (Vaswani et al., 2017). Trained using reinforcement learning, their method outperformed previous methods across a variety of combinatorial problems, representing a major advancement in the field. Kwon et al. (2020) introduced POMO, a reinforcement learning approach which leverages solution symmetries to improve results when compared to the attention model. POMO also introduced an instance augmentation technique, which reformulates a given problem by applying transformations — such as flipping or rotating the Euclidean map of node coordinates — to generate alternative instances that lead to the same solution. This technique forces the exploration of a wider range of potential solutions, enhancing model performance during inference. These works can be considered the backbone of the published research on routing problems, providing inspiration for a wide variety of subsequent studies (Bi et al., 2025; Chalumeau et al., 2023; Fitzpatrick et al., 2024; Grinsztajn et al., 2023; Kim et al., 2022; Kwon et al., 2021; Lei et al., 2022; Lin et al., 2024; Luo et al., 2023; Pirnay and Grimm, 2024; Xin et al., 2020; Zhou et al., 2023, 2024b).

Alternatively, improvement-based methods focus on learning to iteratively refine an initial solution through a structured search process, often drawing inspiration from traditional local search or large neighborhood search algorithms. While these methods are far less prevalent than construction-based approaches, they typically produce higher-quality solutions. However, this comes at the cost of significantly increased inference time. One of the first such approaches in VRP literature, NeuRewriter, was introduced by Chen and Tian (2019). Their approach, trained via reinforcement learning, learns region-picking and rule-picking policies to improve an initially generated solution until convergence. Later, Hottung and Tierney (2020) proposed incorporating a large neighborhood search as the foundation for the search process. They manually designed two destroy operators, while a deep neural network guided the repair process. Ma et al. (2021) introduced a dual-aspect collaborative transformer, which learns separate embeddings for node and positional features. Their model also featured a cyclic encoding technique, which captures the symmetry of VRP problems to enhance generalization. Wu et al. (2022) developed a transformer-based model for solving the TSP and CVRP, which parameterizes a policy to guide the selection of the next solution by integrating 2-opt and swap operators. These studies laid the foundation for many other works, influencing further advancements on the field (Hudson et al., 2022; Kim et al., 2021; Ma et al., 2023; Roberto et al., 2020).

### 2.3. Multi-task learning and transfer learning for VRPs

Most algorithms, whether neural-based or not, are restricted to addressing specific VRP variants. Some machine learning techniques offer greater versatility, enabling the development of models that are not bound to a single task. Among these techniques, multi-task learning and transfer learning hold particular prominence (Pan and Yang, 2010; Zhang and Yang, 2022). Multi-task learning involves training a model simultaneously on data from multiple related but distinct tasks. In this manner, the model can effectively learn shared features and representations across various tasks, improving its generalization ability. In contrast, transfer learning focuses on pre-training a model on a single task and subsequently adapting it to a specific task. This is achieved by loading the pre-trained model’s parameters and making minor adjustments to it, which is faster and more efficient than training a model from the beginning.

While these techniques have been widely studied in computer vision (Yuan et al., 2012) and natural language processing (Dong et al., 2019), their applications in combinatorial optimization remain relatively new. Recently, a few recent studies have begun exploring these methods in this domain, all utilizing reinforcement learning for training. Lin et al. (2024) proposed pre-training a backbone model on a standard TSP and subsequently fine-tuning to adapt to other routing variants, including the orienteering problem, the prize collecting TSP and CVRP. Their approach modified the neural network architecture of the pre-trained model by incorporating additional layers tailored to the unique constraints of each routing variant considered in the fine-tuning phase. Liu et al. (2024) modified the attention model to include an attribute composition block. This technique updates a problem-specific attribute vector, which dynamically activates or deactivates relevant problem features depending on the VRP variant being solved. The model includes four attributes that represent capacity constraints, open routes, time windows, and route limits. Essentially, it functions as a multi-task learning model trained on data from various VRP variants. Zhou et al. (2024a)



aimed to improve generalization by incorporating a mixture-of-experts layer and a gating network. Specifically, the mixture-of-experts consists of multiple specialized sub-models, or “experts”, each one designed to handle different problem variants. The gating network then selects which experts to activate depending on the input, enabling the model to generalize to various tasks more effectively. Finally, [Berto et al. \(2025\)](#) introduced mixed batch training, a technique that enhances convergence by sampling multiple VRP variants within the same training batch. This allows the model to learn from multiple variants simultaneously at each optimization step, improving overall training efficiency.

Despite these contributions, previous works have struggled to achieve strong performance. They are generally outperformed by specialized models trained for specific VRP variants, as well as other traditional optimization methods, such as OR-Tools. This raises a critical concern: if multi-task learning models exhibit a significant performance drop, their practicality in real-world applications becomes challenging to justify. Notably, the transfer learning approach proposed by [Lin et al. \(2024\)](#) achieved good performance. However, this came at the cost of extensive fine-tuning, requiring the same number of epochs as training a model from the beginning. Moreover, their method was limited to the orienteering problem, prize collecting TSP and CVRP, with no exploration of more prevalent VRP variants. Motivated by the aforementioned gaps, we introduce TuneNSearch, a novel transfer learning method pre-trained on MDVRP data and fine-tuned for different VRP variants. TuneNSearch differs from existing work in various aspects: First, to improve the encoding of VRP’s features, we integrate POMO with the residual E-GAT model. While the residual E-GAT model has shown improvements over the attention model, to the best of our knowledge, no prior work has combined it with POMO. We demonstrate that this combination enables a more effective encoding, making a better use of the multiple starting nodes introduced by POMO; Second, while we draw inspiration from [Lin et al. \(2024\)](#), we propose pre-training our model on the MDVRP — a significantly more complex problem than the TSP. This allows the model to learn richer features, facilitating a more effective knowledge transfer across different VRP variants. In addition to generalizing effectively to single-depot variants, TuneNSearch also demonstrates strong performance on various MDVRP variants, tasks that are neglected by current methods; Third, most existing neural-based approaches rely solely on machine learning, with little integration with optimization techniques ([Mazyavkina et al., 2021](#)). As a result, although neural-based methods are generally competitive for solving instances with up to 100 nodes, their generalization to larger instances remains limited. To address this, we incorporate an efficient local search algorithm after model inference, using a diverse set of search operators to iteratively refine solutions. This hybrid approach allows TuneNSearch to generalize more effectively than existing neural-based models across a range of VRP variants, in both randomly generated and benchmark instances. It achieves minimal integrality gaps while adding a small computational burden.

### 3. Preliminaries

In this section we first describe the formulation of the MDVRP and then introduce a brief overview of general neural-based methods for VRPs. After, we present other VRP variants featured in our work, along with their respective constraints.

#### 3.1. MDVRP description

The MDVRP is an extension of the classical VRP, in which multiple depots are considered. This problem can be stated as follows: a set  $\mathcal{D} = \{d_1, d_2, \dots, d_m\}$  of  $m$  depots, and a set  $\mathcal{C} = \{c_1, c_2, \dots, c_n\}$  of  $n$  customers are given. Combined, these sets form a set of nodes  $\mathcal{V} = \mathcal{C} \cup \mathcal{D}$ , where the total number of nodes is  $n + m = g$ . The edge set  $\mathcal{E} = \{e_{ij}\}$ ,  $i, j \in \{0, \dots, g\}$  represents the travel distances between all nodes in the problem. Each instance can be characterized by a graph  $\mathcal{G} = \{\mathcal{V}, \mathcal{E}\}$ . A fleet of vehicles, each with a capacity  $Q$ , is dispatched from all depots to serve the customers. Each customer  $c_i$  has a specific demand  $\delta_i$  and must be visited exactly once by a single vehicle. Once a vehicle completes its route, it must return to its starting depot. The solution tour  $\tau$  represents the sequence of nodes visited in the problem. It consists of multiple sub-tours, where each sub-tour corresponds to the set of nodes visited by an individual vehicle. In other words,  $\tau$  captures the complete routing plan, breaking it down into distinct routes assigned to different

vehicles. A solution is feasible as long as the capacity of each vehicle is not exceeded, and each customer is served exactly once. The objective is to find the optimal tour  $\tau^*$  that minimizes the total distance traveled by all vehicles.

### 3.2. VRPs as a Markov decision process

Most existing neural-based models for VRPs use the reinforcement learning framework for training (Sutton and Barto, 1998). This approach can be formulated as a Markov decision process, which consists of the following key components:

**State:** The state is an observation received by the reinforcement learning agent which represents the current situation of the environment. At each timestep  $t$ , the state  $s_t$  contains the embeddings of all node features, processed by an encoder, along with contextual information about the current partial solution tour.

**Action:** Upon receiving the state  $s_t$ , the agent selects the next action  $a_t$  based on the current state. The action space contains all the nodes that can be added to the current partial solution. A masking mechanism is applied to ensure the feasibility of all solutions. This mechanism removes unfeasible nodes from the candidate actions space at each timestep.

**State transition:** The state transition describes how the environment evolves as the agent picks actions. At each timestep  $t$ , the agent transitions from state  $s_t$  to the next state  $s_{t+1}$  based on the action  $a_t$ . The selected node is then added to the current partial solution, and other constraints are updated, including: the demand of the selected node is marked as fully served, the vehicle’s remaining capacity is reduced by the demand of the selected node, and the masking mechanism is updated to reflect these changes.

**Reward:** The reward is a value used to evaluate the quality of solutions generated by the reinforcement learning agent, acting as a feedback signal to guide the learning process toward minimizing the objective function. At each timestep  $t$ , the agent receives a reward  $r_t = -cost(s_{t+1}, s_t)$  which reflects the negative distance traveled between states  $s_t$  and  $s_{t+1}$ . Once the entire tour is completed, the cumulative reward  $R = -cost(\tau)$  represents the negative total distance traveled in the solution  $\tau$ . The agent’s objective is to maximize its total cumulative reward, which aligns with minimizing the total distance traveled.

**Policy:** To maximize the total cumulative reward, the agent learns a policy, parametrized by an attention-based neural network (policy network) with parameters  $\theta$ . This policy is a function, or model, that maps states to actions. In essence, the agent learns a heuristic to determine how it should select the next action  $a_t$  given the current state  $s_t$ , which is why neural-based methods are often referred to as neural heuristics. At each timestep  $t$ , the policy network takes as input the state  $s_t$  and outputs the probabilities of visiting each node next. The agent then selects the node greedily (i.e., the node with the highest probability) or by sampling (choose an action stochastically based on the probabilities). This process continues until the full tour  $\tau$  is constructed. The probability of constructing a tour  $\tau$  can be expressed as  $p_\theta(\tau|\mathcal{G}) = \prod_{t=1}^Z p_\theta(a_t|\mathcal{G}, a_{<t})$ , where  $a_t$  denotes the selected node,  $a_{<t}$  the current partial solution and  $Z$  is the maximum number of steps. To train the model, most works use the REINFORCE algorithm (Williams, 1992), which is explained in more detail in Section 4.2.

Different from existing approaches, TuneNSearch initially pre-trains the policy network specifically on MDVRP data, which allows the model to establish a solid foundation of knowledge transferable to both single- and multi-depot variants. Then, for each VRP variant, the parameters from the pre-training phase are loaded into the model and a short fine-tuning phase is performed. In this phase, the model undergoes further training using data specific to each VRP variant. This fine-tuning phase is more efficient than training a new model from the beginning for each variant, as the model benefits from the knowledge acquired during pre-training.

### 3.3. VRP variants

The VRP variants solved by TuneNSearch are: i) *CVRP*: considers a single depot, in contrast to the multiple depots considered in MDVRP; ii) *VRP with backhauls* (VRPB): in the standard CVRP, each customer  $c_i$  has a demand  $\delta_i > 0$ , referred to as linehaul customer. However, in practice, some customers can have a negative demand, known as backhaul customers, requiring the vehicle to load goods rather than unloading them. We consider a mixed VRPB, allowing vehicles to visit both linehaul and backhaul customers

without a strict order; iii) *VRP with duration limit* (VRPL): in this variant, the length of each route cannot surpass a predefined threshold limit; iv) *Open VRP* (OVRP): in the OVRP, vehicles do not need to return to the depot after completing their route; v) *VRP with time windows* (VRPTW): in the VRPTW, each node has a designated time window, during which service must be made, as well as a service time, representing the time needed to complete service at that location; vi) *Traveling salesman problem* (TSP): the TSP is a simplified form of the CVRP that involves only a single route. In this problem, there is no depot, and nodes have no demands. Each node must be visited exactly once, and the vehicle (or salesman) must return to the starting node at the end of the route. We note that the constraints outlined above can also be applied to the MDVRP, instead of the CVRP. For more details on the generation of instances specific to all the described variants, we refer readers to [Appendix B](#).

## 4. Methodology

In this section, we formally describe our proposed method. Our work makes significant advances in two key areas: the development of a method with great generalization capability over different VRP variants, and the improvement of the inference process via the intersection of operations research with artificial intelligence methods. To achieve this, we do the following: i) Design of a novel model architecture combining POMO and the residual E-GAT encoder; ii) Implementation of a pre-training and fine-tuning framework designed to facilitate adaptation to the most common VRP variants; iii) Integration of a local search algorithm which applies different search operators to iteratively improve the solutions found by the neural-based model. The following sections detail each of these components.

### 4.1. Model architecture

Below we outline the architecture of TuneNSearch, which is built upon POMO. Our method incorporates the residual E-GAT in the encoder, which has previously shown performance improvements over the attention model ([Lei et al., 2022](#)). Unlike standard attention-based encoders that rely solely on node coordinates, the residual E-GAT extends the original graph attention network ([Velićković et al., 2018](#)) by incorporating the information of edges  $e_{ij} \in \mathcal{E} \forall i, j \in \{0, \dots, g\}$  and introducing residual connections between consecutive layers. These enhancements allow the model to better capture the information of graph structures, deriving efficient representations and more accurate attention coefficients. When paired with POMO’s multiple starting nodes sampling strategy, this enhanced encoding allows the model to evaluate diverse solution trajectories from different starting points with more precision. The distance-aware attention mechanism ensures that each rollout receives more contextually relevant information, helping the model converge to higher-quality solutions. To the best of our knowledge, this is the first time the residual E-GAT encoder is combined with POMO. Fig. 1 presents an illustration of the encoder-decoder structure of TuneNSearch. The model first encodes the features of depots, customers, and edge distances using a residual E-GAT. The resulting embeddings, along with contextual information about the partial solution tour, are then passed through a multi-head attention (MHA) layer. Finally, a single-head attention (SHA) layer, followed by a softmax function, calculates the probability of selecting each node next.

#### 4.1.1. Encoder details

Our encoder first embeds the features of all nodes in the problem to a  $h_x$ -dimensional vector space through a fully connected layer. Specifically, each depot  $d_j \in \mathcal{D}$  is characterized by features  $n_j^d$ , which include its two-dimensional coordinates. On the other hand, each customer  $c_i \in \mathcal{C}$  has features  $n_i^c$ , which not only contain its coordinates, but also the demand information and the early and late time windows. These features are passed through embedding layers separately for depots and customers. The result is a set of embedded vectors  $\{\hat{n}_j^d \in \mathbb{R}^{h_x} \mid j = 1, \dots, m\}$  for depots and  $\{\hat{n}_i^c \in \mathbb{R}^{h_x} \mid i = 1, \dots, n\}$  for customers, as shown in Equations 1 and 2. These vectors are then stacked to form  $E^d \in \mathbb{R}^{m \times h_x}$  and  $E^c \in \mathbb{R}^{n \times h_x}$ . After, they are concatenated into  $x^{(0)} \in \mathbb{R}^{g \times h_x}$ , as demonstrated in Equation 3. We also embed the edge



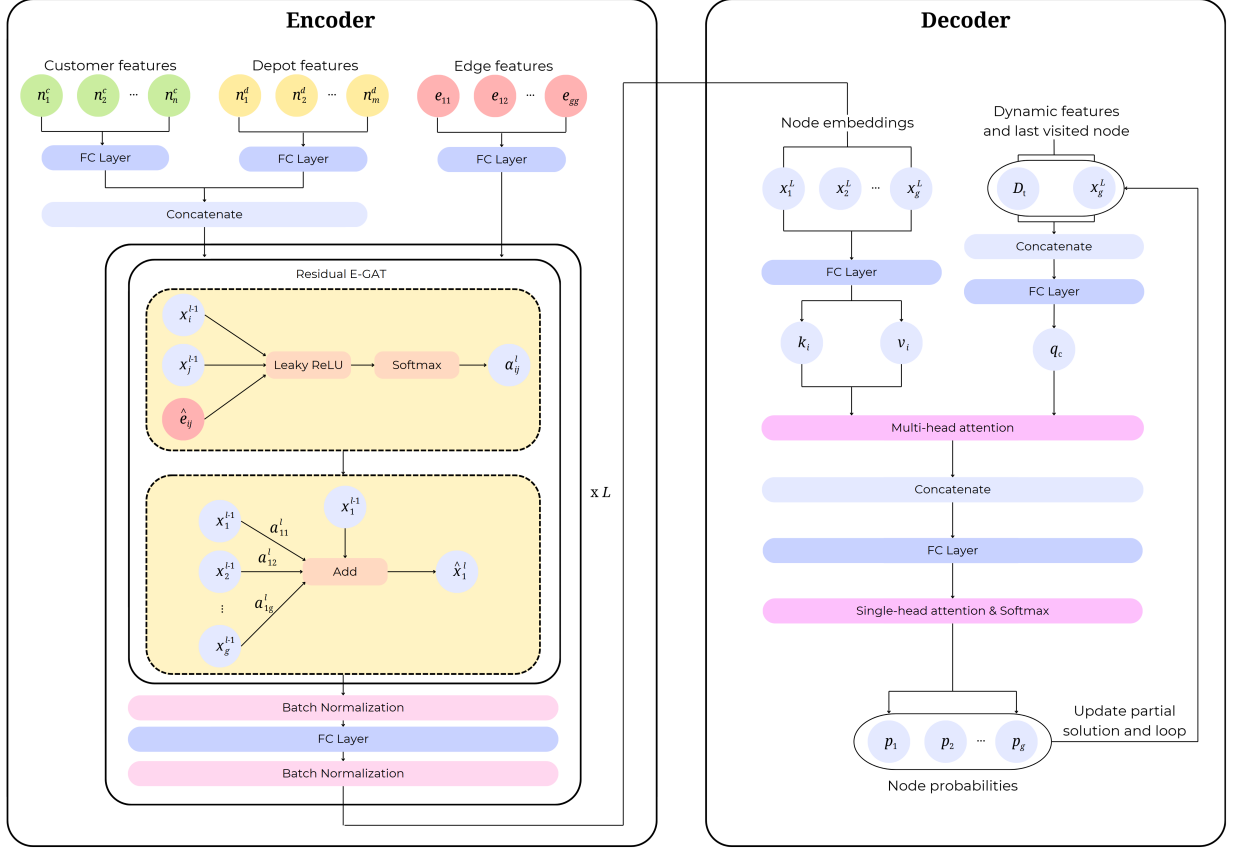


Figure 1: Encoder-decoder structure of TuneNSearch.

features, which represent the Euclidean travel distances  $e_{ij}$ ,  $i, j \in \{1, 2, \dots, g\}$ , into a  $h_e$ -dimensional vector space, as described in Equation 4.

$$\hat{n}_i^c = A_0 n_i^c + b_0, \quad \forall i \in \{1, \dots, n\} \quad (1)$$

$$\hat{n}_j^d = (A_1 n_j^d + b_1), \quad \forall j \in \{1, \dots, m\} \quad (2)$$

$$x^{(0)} = \text{concat}(E^d, E^c) = \{x_1^{(0)}, \dots, x_g^{(0)}\} \quad (3)$$

$$\hat{e}_{ij} = (A_2 e_{ij} + b_2), \quad \forall i, j \in \{1, 2, \dots, g\} \quad (4)$$

After this initial transformation, both  $x^{(0)}$  and  $\hat{e} = \hat{e}_{11}, \hat{e}_{12}, \dots, \hat{e}_{gg}$  are used as inputs to a residual E-GAT module with  $L$  layers. Here, the attention coefficient  $\alpha_{ij}^l$  indicates the influence of the features of the node indexed by  $j$  on the node indexed by  $i$ , at layer  $l \in \{1, 2, \dots, L\}$ . The coefficient  $\alpha_{ij}^l$  can be calculated according to Equation 5:

$$\alpha_{ij}^l = \frac{\exp(\text{LeakyReLU}(a^{lT} [W_1^l(x_i^{(l-1)} || x_j^{(l-1)} || \hat{e}_{ij})]))}{\sum_{k=0}^g \exp(\text{LeakyReLU}(a^{lT} [W_1^l(x_i^{(l-1)} || x_k^{(l-1)} || \hat{e}_{ik})]))} \quad (5)$$

where  $a^l$  and  $W_1^l$  are learnable weight matrices.

Then, a residual connection between consecutive layers is applied, in which the output at layer  $l$ , for node indexed by  $i$ , can be represented as indicated in Equation 6:

$$\hat{x}_i^{(l)} = \left( \sum_{k=0}^g \alpha_{ik}^l W_2^l x_i^{(l-1)} \right) + x_i^{(l-1)} \quad (6)$$

where  $W_2^l$  is also a learnable matrix.

Lastly, after each E-GAT layer, the output also passes through two batch normalization and one fully connected layer. See Equations 7 and 8.

$$\hat{x}_i = \text{BatchNorm}^l(x_i^{(l-1)} + \hat{x}_i^{(l)}) \quad (7)$$

$$x_i^{(l)} = \text{BatchNorm}^l(\hat{x}_i + FC(\hat{x}_i)) \quad (8)$$

#### 4.1.2. Decoder details

Following the approach proposed by Kool et al. (2019), we apply an MHA layer followed by a SHA layer for the decoder. First, the decoder takes the initial node embeddings  $x_i^{(L)}$  (we omit the  $(L)$  term for better readability) and sets the keys and values for all  $H$  heads of the MHA, as indicated in Equations 9 and 10:

$$v_i = W^V x_i, \forall i \in \{1, 2, \dots, g\} \quad (9)$$

$$v = k_i = W^V = K x_i, \forall i \in \{1, 2, \dots, g\} \quad (10)$$

where  $W^V, W^K \in \mathbb{R}^{h_v \times h_x}$  are learnable matrices and  $h_v = (h_x/H)$ , with  $v_i, k_i \in \mathbb{R}^{h_v}$ .

To generate the query vector  $q_c$ , the embeddings of the currently selected node ( $x_{i_t}$ , at timestep  $t$ ) are concatenated with dynamic features  $D_t$ , as described in Equation 11.

$$q_c = W^Q \text{concat}(x_{i_t}, D_t) \quad (11)$$

where  $W^Q \in \mathbb{R}^{h_v \times h_x}$  is a learnable matrix. The features  $D_t$  include the vehicle load at timestep  $t$ , the elapsed time, the length of the current route and a Boolean to indicate whether routes are open or not. For the TSP, we do not perform this concatenation operation, as the problem is solely defined by node coordinates. Therefore, we exclude the 4 neurons associated with the dynamic features  $D_t$ .

The node compatibilities  $u_{ci}, \forall i \in \{1, 2, \dots, g\}$  are then calculated through the query vector  $q_c$  and the key vector  $k_i$ , as shown in Equation 12:

$$u_{ci} = C \cdot \tanh(q_c^T k_i) \quad (12)$$

where the results are clipped within  $[-C, C]$ . Furthermore, the compatibility of infeasible nodes is set to  $-\infty$  to guarantee that only feasible solutions are generated. Lastly, the probability  $p_i, \forall i \in \{1, 2, \dots, g\}$  of each node is computed through a softmax function, as indicated in Equation 13.

$$p_i = \frac{e^{u_{ci}}}{\sum_{j=1}^g e^{u_{cj}}} \quad (13)$$

#### 4.2. Model training

To train our model, we used the REINFORCE algorithm (Williams, 1992), which is a fundamental policy gradient method used in reinforcement learning. In particular, we use the REINFORCE with shared baselines algorithm, following the approach of POMO (Kwon et al., 2020), where multiple trajectories are sampled with  $N$  different starting nodes. To this end, the total rewards  $R(\tau^1, \dots, \tau^N)$  are calculated for each solution sampled. For a batch with  $B$  different instances, gradient ascent is used to maximize the total expected return  $J$ , as indicated in Equation 14:

$$\nabla_{\theta} J(\theta) = \frac{1}{BN} \sum_{i=1}^B \sum_{j=1}^N (R(\tau_i^j) - b_i) \nabla_{\theta} \log p_{\theta}(\tau_i^j) \quad (14)$$

where  $\theta$  is the set of model parameters and  $p_{\theta}(\tau_i^j)$  is the probability of trajectory  $\tau_i^j$  being selected. Furthermore,  $b_i$  is a shared baseline calculated according to Equation 15:

$$b_i = \frac{1}{N} \sum_{j=1}^N R(\tau_i^j), \forall i \in \{1, \dots, B\} \quad (15)$$

Algorithm 1 outlines the REINFORCE with shared baselines algorithm in more detail. First, the policy network is initialized with a random set of parameters  $\theta$ . Then, training begins by looping over  $E$  epochs, each comprising  $T$  steps. At each step, a batch of  $B$  random training instances is sampled, and for each instance,  $N$  starting nodes are selected. For all experiments, we set  $N$  as  $g - 1$ , consistent with prior work (Kwon et al., 2020; Li et al., 2024). From these nodes, trajectories are sampled through the model architecture explained in Section 4.1. Then, the shared baseline is calculated (Equation 15), which is used to compute the policy gradients  $\nabla_{\theta} J(\theta)$  (Equation 14). Lastly, the set of parameters  $\theta$  is updated through gradient ascent, scaled by a learning rate  $\eta$ .

---

**Algorithm 1** REINFORCE with shared baselines (Kwon et al., 2020)

---

**Require:** Number of epochs  $E$ , batch size  $B$ , steps per epoch  $T$

- 1: Initialize policy network with parameters  $\theta$
  - 2: **for**  $epoch = 1$  **to**  $E$  **do**
  - 3:   **for**  $step = 1$  **to**  $T$  **do**
  - 4:     Randomly sample set  $\mathcal{S} = \{\mathcal{G}_1, \mathcal{G}_2, \dots, \mathcal{G}_B\}$  with  $B$  training instances
  - 5:     Select  $N$  starting nodes for each instance  $\mathcal{G}_i$ ,  $i \in \{1, \dots, B\}$
  - 6:     Using the selected starting nodes, sample trajectories  $\tau_i^j$ ,  $\forall i \in \{1, \dots, B\}, \forall j \in \{1, \dots, N\}$
  - 7:      $b_i \leftarrow \frac{1}{N} \sum_{j=1}^N R(\tau_i^j)$ ,  $\forall i \in \{1, \dots, B\}$
  - 8:      $\nabla_{\theta} J(\theta) \leftarrow \frac{1}{BN} \sum_{i=1}^B \sum_{j=1}^N (R(\tau_i^j) - b_i) \nabla_{\theta} \log p_{\theta}(\tau_i^j)$
  - 9:      $\theta \leftarrow \theta + \eta \nabla_{\theta} J(\theta)$
  - 10:   **end for**
  - 11: **end for**
- 

#### 4.3. Pre-training and fine-tuning process

With the architecture described above, we pre-train a backbone model for 100 epochs, similarly to the framework proposed by Lin et al. (2024). However, rather than training on TSP data, we use MDVRP instances. This choice is motivated by the higher complexity of the MDVRP, which enables the model to learn richer node representations in comparison to the TSP. Besides, pre-training on the MDVRP also offers advantages over pre-training on the CVRP by exposing the model to a multi-depot structure. As a result, our model generalizes as well as a CVRP pre-trained model on single-depot variants, while achieving significantly better performance on multi-depot tasks.

Additionally, in contrast to Lin et al. (2024), during pre-training we incorporate all dynamic features  $D_t$  relevant across all VRP variants considered. Rather than introducing problem-specific modules, this approach allows us to fine-tune the model for each VRP variant without modifying the neural network architecture. This avoids the loss of potentially useful knowledge when transitioning between variants. The only structural change occurs when adapting the model for the TSP, as it is the simplest routing problem we address. The TSP differs from other VRP variants since it involves only node coordinates, with no demands, time windows, or additional constraints. For TSP-specific fine-tuning, we modify the encoder by removing the fully connected layer responsible for embedding customer features, leaving only depot (characterized solely by coordinates) and edge features.

For the fine-tuning phase, we load the parameters from the pre-trained MDVRP model and train it for an additional 20 epochs on randomly generated instances, tailored to each specific VRP variant. We use the same hyper-parameters as in the pre-training phase. The dynamics of the pre-training and fine-tuning stages of TuneNSearch are illustrated in Fig. 2. We note that besides the main variants described in Section 3.3, TuneNSearch can be extended to any combination of VRP constraints. For example, it can handle combinations like the MDVRP with time windows, open routes and backhauls, allowing it to tackle more complex routing problems.

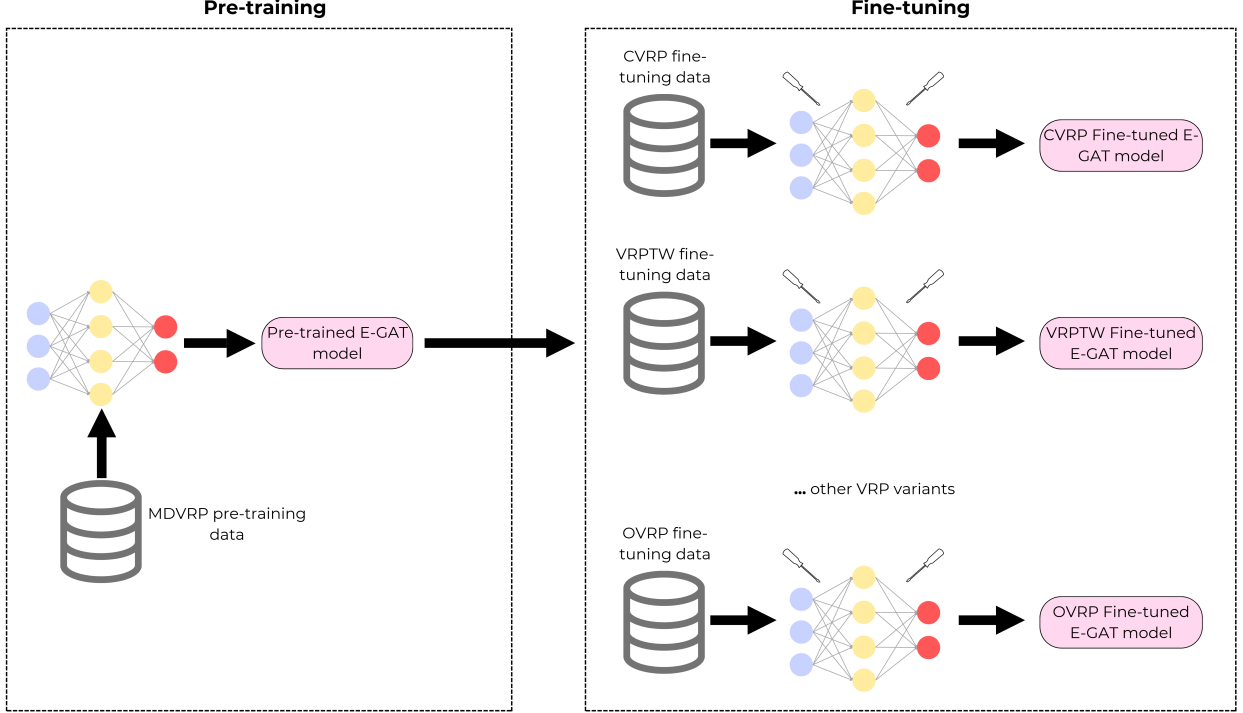


Figure 2: TuneNSearch pre-training and fine-tuning overview.

#### 4.4. Local search algorithm

Despite the recent interest in using neural-based techniques to solve VRPs, there remains a limited integration between operations research and machine learning methods in the current literature. Bridging this gap offers an opportunity to combine the strengths of both fields, enabling the development of more powerful and efficient algorithms. To refine the solutions obtained by the neural-based model, we designed an efficient local search algorithm employed after inference, inspired by different existing methods.

This algorithm involves applying various operators within restricted neighborhoods of predefined size. Following Vidal (2022), we define the neighborhood size as 20, which allows for an efficient exploration of the granular neighborhood. A granular neighborhood is a restricted subset of the solution space that is defined based on proximity criteria. Rather than evaluating moves across the entire problem domain, the search is confined to carefully selected neighborhoods of limited size, where meaningful improvements are more likely to be found. Specifically, the chosen operators apply moves restricted to node pairs  $(a, b)$ , where  $b$  is one of the 20 closest nodes to  $a$ . All moves are evaluated within different neighborhoods, and any improvement in the cost function is immediately applied. The search procedure terminates once no further improvements to the cost function are possible, which occurs after all applicable operators and moves have been applied. We adopt the same set of operators as Wouda et al. (2024), which were selected due to their ability to

effectively explore the solution space while maintaining computational efficiency. Each operator targets different aspects of the solution structure, ensuring a well-balanced and diverse set of moves to improve the solution quality. The chosen operators include:

- **(X, M)-exchange:** involves swapping  $X$  customers from a route, starting at a designated node, with a segment of  $M$  customers (where  $0 \leq M \leq X$ ) starting at a different node. Importantly, the two segments must not overlap, ensuring that the exchange modifies the routes without duplicating any customers.
- **MoveTwoClientsReversed:** involves selecting two customers from a given route and moving them to a different position in a reversed order, essentially functioning as a reversed (2, 0)-exchange.
- **2-OPT:** iteratively removes two edges from a route and reconnects the resulting paths in a different configuration.
- **RELOCATE\*:** identifies and executes the most optimal relocation where an individual customer is removed from one route and inserted into the best possible position of another route.
- **SWAP\*:** evaluates and executes the most beneficial exchange of two customers between two routes, positioning each customer in the optimal location within the other route. Unlike a traditional swap, this operator exchanges two customers from different routes by inserting them into any position on the opposite route, rather than directly swapping them in place.

In more detail, the local search algorithm (see Algorithm 2) begins with an initial solution  $\tau$ , which is the best solution obtained from the E-GAT model. The algorithm assumes a fixed number of iterations  $I$ , and solutions are represented as sequences of visited nodes. The best distance ( $BD$ ) is initialized as the cost of  $\tau$ , and the best solution ( $BS$ ) is set to  $\tau$ . Before the iterative process starts, the algorithm explores the neighborhood of  $\tau$  using the *Search* function. This function applies all the operators and moves explained above to identify potential improvements to the solution. If a better solution is found during this step, both  $BD$  and  $BS$  are updated accordingly. After that, in each iteration, to escape local minimum, an offspring solution ( $OS$ ) is generated using the *Crossover* function. This function takes as parents the current  $BS$  and a randomly generated solution, created with the *MakeRandom* function. Here, we use the selective route exchange crossover operator proposed by Nagata and Kobayashi (2010). Then, the neighborhood of  $OS$  is explored through the *Search* function. If the resulting solution is infeasible, the algorithm repairs it using the *Fix* function, which applies the search operators again while considering only feasible moves. Finally, if the new solution's cost is better than the current  $BD$ , the algorithm updates  $BD$  and  $BS$ . This process is repeated for  $I$  iterations.

Fig. 3 depicts an overview of the complete inference process, coupled with the local search algorithm. The process begins with the trained E-GAT model solving a given testing instance, generating an initial solution represented as sub-tours (or routes). This solution is then improved by the local search algorithm, which explores the solution space. Finally, the best overall solution found is returned.



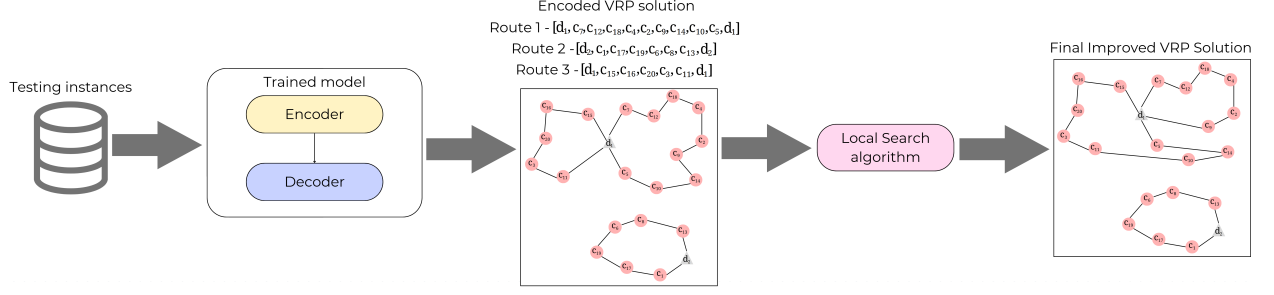


Figure 3: Overview of the inference process of TuneNSearch.

---

**Algorithm 2** Local Search Algorithm

---

**Require:** Number of iterations  $I$ , initial solution  $\tau$

```

1:  $BD \leftarrow Cost(\tau)$ 
2:  $BS \leftarrow \tau$ 
3:  $\tau' \leftarrow Search(\tau)$ 
4: if  $Cost(\tau') < BD$  then
5:    $BD \leftarrow Cost(\tau')$ 
6:    $BS \leftarrow \tau'$ 
7: end if
8: for  $iteration = 1$  to  $I$  do
9:    $OS \leftarrow Crossover(BS, MakeRandom())$ 
10:   $\tau \leftarrow Search(OS)$ 
11:  if not  $IsFeasible(\tau)$  then
12:     $\tau \leftarrow Fix(\tau)$ 
13:  end if
14:  if  $Cost(\tau) < BD$  then
15:     $BD \leftarrow Cost(\tau)$ 
16:     $BS \leftarrow \tau$ 
17:  end if
18: end for

```

---

## 5. Experimental results

In this section, we verify and demonstrate the performance of TuneNSearch through a series of extensive experiments. In addition to the MDVRP, we consider the primary VRP variants described in Section 3.3. Our models were implemented using PyTorch (Paszke et al., 2017), and all neural-based experiments were conducted on a machine with 45GB of RAM, an Intel Xeon Gold 5315Y and an Nvidia Quadro RTX A6000. The baselines PyVRP and OR-Tools Routing library were executed on a machine with 32 GB of RAM and an Intel Core i9-13900. We note that the use of different computers does not affect the fairness of the comparison, as PyVRP and OR-Tools are not neural-based frameworks and therefore do not benefit from GPU acceleration.

**Baselines:** To evaluate the performance of TuneNSearch, we compared it against four state-of-the-art baseline approaches: PyVRP, OR-Tools Routing library, MD-MTA and POMO. For PyVRP and OR-Tools, we set time limits of 300, 600 and 1800 seconds for problems of sizes  $n = 20, 50, 100$ , respectively. Both methods were parallelized across 32 CPU cores, following prior research (Kool et al., 2019; Zhou et al., 2024a).

**Training and hyper-parameters:** We consider three MDVRP models trained on instances of sizes  $n = 20, 50, 100$ , where the number of depots ( $m$ ) was set to 2, 3, and 4, respectively. Each model was

trained for 100 epochs, with one epoch consisting of 320000 training instances for  $n \in 20, 50$ , and 160000 for  $n = 100$ . Batch sizes were set to 2000, 500 and 120 for each instance size, respectively. When fine-tuning our pre-trained MDVRP model, we consider 20 additional epochs for each VRP variant. For all baselines, we maintained the original hyper-parameters from their respective works. For TuneNSearch, we set the hidden dimension at  $h_x = 256$  and the hidden edge dimension at  $h_e = 32$ . The number of encoder layers is  $L = 5$ , and the fully connected layer in the encoder has a hidden dimension of 512. The number of heads in the MHA decoder is  $H = 16$ , and the tanh clip size was set to 10, according to Bello et al. (2017). We employed the Adam optimizer (Kingma and Ba, 2015) with a learning rate of  $\eta = 10^{-4}$ . We provide a sensitivity analysis of key hyper-parameters in Appendix A.

### 5.1. Computational results on randomly generated instances

Table 1 provides a comparison between our pre-trained MDVRP model and MD-MTA, as well as between POMO (specialized for each specific VRP variant) and our fine-tuned models. The evaluation is based on 1280 randomly generated instances per problem and considers three key metrics: the average total distance traveled (Obj.), the average gap (Gap) compared to the best solutions found across all evaluated methods, and the computational time (Time) taken to solve all instances. The best results — i.e., the lowest average total distance traveled and gap (relative to PyVRP) — are highlighted in **bold**.

For all neural-based methods, we used a greedy decoding with x8 instance augmentation (Kwon et al., 2020), except for MD-MTA, which we applied the enhanced depot rotation augmentation designed by Li et al. (2024). Additionally, we evaluated TuneNSearch under two other configurations: i) with the local search applied post-inference (labeled *ls.*); ii) with local search but without x8 instance augmentation (labeled *ls. + no aug.*). In both configurations, the local search was performed for 50 iterations.

For MDVRP instances, TuneNSearch consistently outperformed MD-MTA across all three problem sizes, even without employing the local search. When the local search is applied, the improvements became more pronounced, achieving minimal integrality gaps compared to PyVRP. Notably, even without x8 augmentation, the application of the local search significantly enhanced performance, allowing our model to perform better than OR-Tools and MD-MTA.

For other VRP variants, TuneNSearch generally outperformed POMO, and even OR-Tools in many cases, achieving results close to PyVRP. Similar to the MDVRP results, applying the local search led to substantial performance gains. We can also notice that the additional computational burden associated with the local search is minimal, as TuneNSearch runs for a fraction of the time required by PyVRP and OR-Tools.

We also conducted an additional set of experiments — using the same 100-node instances of Table 1 — where PyVRP and OR-Tools were limited to a similar computational time budget to that of TuneNSearch. Note that, in some variants, OR-Tools required more time than PyVRP and TuneNSearch, as this was the minimum time necessary to find a feasible solution. For TuneNSearch, we report results with the local search algorithm after inference. As shown in Table 2, when running under a comparable time budget, TuneNSearch outperformed PyVRP in 5 out of the 7 tested variants, achieving a lower average objective value overall. In contrast, OR-Tools did not prove to be competitive, performing significantly worse than both PyVRP and TuneNSearch in all variants. These results suggest that, in time-constrained applications, TuneNSearch is the most viable alternative.

To further support our results, we conducted a means plot, and a 95% confidence level Tukey’s honestly significance difference (HSD) test on all 1280 generated instances for problems of sizes  $n = 100$ . The results, presented in Fig. 4, reveal that TuneNSearch performs statistically better than POMO in nearly all variants. When compared to OR-Tools, TuneNSearch demonstrates superior performance in three variants (MDVRP, CVRP, and VRPL), with no statistically significant difference in the remaining tasks. In comparison to PyVRP, TuneNSearch shows no significant difference in two variants (CVRP and VRPL), but performs statistically worse in the others. Under a restricted time budget, TuneNSearch significantly outperforms OR-Tools across all variants. When compared to PyVRP, TuneNSearch shows no statistically significant difference in any of the variants, except for TSP, where it performs better. However, TuneNSearch exhibits a lower average objective value in 5 out of 7 variants.

Table 1: Experimental results on all VRP variants (\* represents 0.000 % gap).

	Method	$n = 20$			$n = 50$			$n = 100$		
		Obj.	Gap	Time (m)	Obj.	Gap	Time (m)	Obj.	Gap	Time (m)
MDVRP	PyVRP	4.494	*	200.134	7.489	*	401.243	11.345	*	1200.436
	OR-Tools	<b>4.494</b>	*	200.026	7.523	0.454 %	400.043	11.637	2.574 %	1200.160
	MD-MTA	4.548	1.202 %	0.104	7.679	2.537 %	0.237	11.797	3.984 %	0.944
	Ours	4.518	0.534 %	0.055	7.637	1.976 %	0.146	11.744	3.517 %	0.535
	Ours (ls.)	4.495	0.022 %	0.263	<b>7.521</b>	<b>0.427 %</b>	1.017	<b>11.521</b>	<b>1.551 %</b>	3.270
	Ours (ls. + no aug.)	4.496	0.045 %	0.241	7.535	0.614 %	0.908	11.582	2.089 %	2.784
CVRP	PyVRP	4.977	*	200.128	9.392	*	401.465	16.124	*	1200.323
	OR-Tools	4.977	*	200.023	9.468	0.809 %	400.036	16.613	3.033 %	1200.038
	POMO	4.991	0.281 %	0.040	9.502	1.171 %	0.089	16.531	2.524 %	0.296
	Ours	4.992	0.301 %	0.050	9.494	1.086 %	0.133	16.430	1.898 %	0.484
	Ours (ls.)	4.977	*	0.257	<b>9.422</b>	<b>0.319 %</b>	1.045	<b>16.303</b>	<b>1.110 %</b>	3.310
	Ours (ls. + no aug.)	4.978	0.020 %	0.244	9.435	0.458 %	0.964	16.370	1.526 %	2.920
VRPB	PyVRP	4.551	*	200.119	8.119	*	401.439	13.450	*	1200.328
	OR-Tools	<b>4.551</b>	*	200.023	<b>8.144</b>	<b>0.308 %</b>	400.031	13.766	2.349 %	1200.128
	POMO	4.583	0.703 %	0.041	8.274	1.909 %	0.085	13.938	3.628 %	0.294
	Ours	4.578	0.593 %	0.043	8.285	2.045 %	0.128	<b>13.867</b>	<b>3.100 %</b>	0.451
	Ours (ls.)	4.554	0.066 %	0.243	8.159	0.493 %	0.996	<b>13.660</b>	<b>1.561 %</b>	3.481
	Ours (ls. + no aug.)	4.554	0.066 %	0.212	8.168	0.604 %	0.915	13.717	1.985 %	2.861
VRPL	PyVRP	4.998	*	200.124	9.349	*	401.492	16.138	*	1200.318
	OR-Tools	4.998	*	200.024	9.420	0.759 %	400.037	16.644	3.135 %	1200.045
	POMO	5.022	0.480 %	0.084	9.457	1.155 %	0.134	16.507	2.287 %	0.364
	Ours	5.017	0.380 %	0.099	9.451	1.091 %	0.181	16.448	1.921 %	0.556
	Ours (ls.)	4.998	*	0.295	<b>9.378</b>	<b>0.310 %</b>	1.084	<b>16.324</b>	<b>1.153 %</b>	3.366
	Ours (ls. + no aug.)	4.999	0.020 %	0.276	9.391	0.449 %	0.976	16.394	1.586 %	2.976
OVRP	PyVRP	3.480	*	200.138	6.150	*	401.387	9.949	*	1200.345
	OR-Tools	<b>3.480</b>	*	200.022	<b>6.161</b>	<b>0.179 %</b>	400.038	<b>10.118</b>	<b>1.699 %</b>	1200.128
	POMO	3.498	0.517 %	0.041	6.315	2.683 %	0.090	10.484	5.377 %	0.295
	Ours	3.499	0.546 %	0.050	6.290	2.276 %	0.134	10.404	4.573 %	0.487
	Ours (ls.)	3.481	0.029 %	0.239	6.171	0.341 %	0.938	10.126	1.779 %	3.022
	Ours (ls. + no aug.)	3.481	0.029 %	0.196	6.175	0.407 %	0.807	10.147	1.990 %	2.671
VRPTW	PyVRP	7.654	*	200.120	14.545	*	401.586	24.692	*	1200.327
	OR-Tools	<b>7.654</b>	*	200.024	<b>14.724</b>	<b>1.231 %</b>	400.055	25.614	3.734 %	1201.444
	POMO	7.834	2.352 %	0.040	15.179	4.359 %	0.095	26.239	6.265 %	0.345
	Ours	7.813	2.077 %	0.052	15.155	4.194 %	0.143	26.163	5.957 %	0.550
	Ours (ls.)	7.673	0.248 %	0.332	14.762	1.492 %	1.497	<b>25.586</b>	<b>3.621 %</b>	4.532
	Ours (ls. + no aug.)	7.680	0.340 %	0.289	14.776	1.588 %	1.407	25.617	3.746 %	4.072
TSP	PyVRP	3.829	*	200.127	5.692	*	401.941	7.757	*	1200.387
	OR-Tools	3.829	*	200.020	<b>5.692</b>	*	400.036	<b>7.768</b>	<b>0.142 %</b>	1200.023
	POMO	3.829	*	0.037	5.697	0.088 %	0.078	7.828	0.915 %	0.257
	Ours	3.829	*	0.045	5.700	0.141 %	0.116	7.824	0.864 %	0.421
	Ours (ls.)	3.829	*	0.204	5.693	0.018 %	0.745	7.783	0.335 %	2.588
	Ours (ls. + no aug.)	3.829	*	0.166	5.698	0.105 %	0.662	7.819	0.799 %	2.214
Average	PyVRP	4.855	*	200.127	8.677	*	401.508	14.208	*	1200.352
	OR-Tools	<b>4.855</b>	*	200.023	8.733	0.652 %	400.039	14.594	2.720 %	1200.281
	POMO (+MD-MTA)	4.901	0.948 %	0.055	8.872	2.251 %	0.115	14.761	3.890 %	0.327
	Ours	4.892	0.774 %	0.056	8.859	2.101 %	0.140	14.697	3.444 %	0.498
	Ours (ls.)	4.858	0.071 %	0.262	<b>8.729</b>	<b>0.609 %</b>	1.046	<b>14.472</b>	<b>1.858 %</b>	3.367
	Ours (ls. + no aug.)	4.860	0.100 %	0.232	8.740	0.728 %	0.948	14.521	2.203 %	2.928

## 5.2. Computational results on benchmark instances

To evaluate the generalization of TuneNSearch, we tested its performance on benchmark instances for the MDVRP, VRPL, CVRP, TSP and VRPTW, as detailed in Tables 3, 4, 5, 6 and 7. All tasks were solved greedily with x8 instance augmentation, followed by the local search algorithm (250 iterations, as we solved individual instances in this subsection). For all variants, we used models trained with instances of size  $n = 100$ . Additionally, we provide the solutions generated by TuneNSearch for each instance as supplementary material.

For the MDVRP, we assessed our model on Cordeau’s dataset (Cordeau et al., 1997), which includes 23 problems: instances 1-7 were proposed by Christofides and Eilon (1969), instances 8-11 by Gillett and Johnson (1976) and instances 12-23 by Chao et al. (1993). We compared our results to the best-known

Table 2: Experimental results on all VRP variants under equal computational time budget.

Method		$n = 100$		
		Obj.	Gap	Time (m)
MDVRP	PyVRP	11.601	2.256 %	3.505
	OR-Tools	12.541	10.538 %	8.052
	Ours (ls.)	<b>11.521</b>	<b>1.151 %</b>	3.270
CVRP	PyVRP	16.345	1.371 %	3.501
	OR-Tools	17.669	9.582 %	3.363
	Ours (ls.)	<b>16.303</b>	<b>1.110 %</b>	3.310
VRPB	PyVRP	<b>13.640</b>	<b>1.155 %</b>	3.495
	OR-Tools	14.664	9.026 %	5.361
	Ours (ls.)	13.660	1.561 %	3.481
VRPL	PyVRP	16.362	1.388 %	3.501
	OR-Tools	17.576	8.911 %	4.698
	Ours (ls.)	<b>16.324</b>	<b>1.153 %</b>	3.366
OVRP	PyVRP	<b>10.031</b>	<b>0.824 %</b>	3.509
	OR-Tools	10.875	9.307 %	5.371
	Ours (ls.)	10.126	1.779 %	3.022
VRPTW	PyVRP	25.964	5.151 %	4.833
	OR-Tools	26.923	9.035 %	9.408
	Ours (ls.)	<b>25.586</b>	<b>3.621 %</b>	4.532
TSP	PyVRP	7.938	2.333 %	2.818
	OR-Tools	8.002	3.158 %	2.693
	Ours (ls.)	<b>7.783</b>	<b>0.335 %</b>	2.588
Average	PyVRP	14.554	2.435 %	3.594
	OR-Tools	15.464	8.840 %	5.564
	Ours (ls.)	<b>14.472</b>	<b>1.858 %</b>	3.367

solutions (BKS) for these instances, reported by [Sadati et al. \(2021\)](#). TuneNSearch was compared against the MD-MTA model, using a greedy decoding along with the enhanced depot rotation augmentation suggested in their work.

For the VRPL, CVRP, TSP and VRPTW, we evaluated TuneNSearch using instances from CVRPLIB (Set-Golden, Set-X and Set-Solomon) ([Golden et al., 1998](#); [Solomon, 1987](#); [Uchoa et al., 2017](#)) and TSPLIB ([Reinelt, 1991](#)). For the CVRP and TSP, we compared our results with those presented by [Zhou et al. \(2023\)](#), which include POMO ([Kwon et al., 2020](#)), the adaptative multi-distribution knowledge distillation model (AMDKD-POMO) ([Bi et al., 2022](#)), the meta-learning approach (Meta-POMO) proposed by [Manchanda et al. \(2023\)](#), and the omni-generalizable model (Omni-POMO) ([Zhou et al., 2023](#)). For the VRPTW, our results were compared against those reported by [Zhou et al. \(2024a\)](#). For the VRPL, since it is a variant not commonly evaluated on benchmark instances, we provide the results obtained by POMO.

In MDVRP benchmarks, TuneNSearch consistently outperformed the MD-MTA in all tested instances. For the VRPL, CVRP, TSP and VRPTW, TuneNSearch outperformed the other models in most instances, often by a significant margin. These results demonstrate the effectiveness of our approach and the implementation of the local search procedure.

Furthermore, these findings underscore the strong generalization capabilities of TuneNSearch across various tasks, distributions, and problem sizes, addressing a long-standing challenge in neural-based methods. As shown in Tables 3 and 4, TuneNSearch demonstrates strong scalability as the problem size increases, maintaining computational efficiency while achieving solutions close to the BKS.

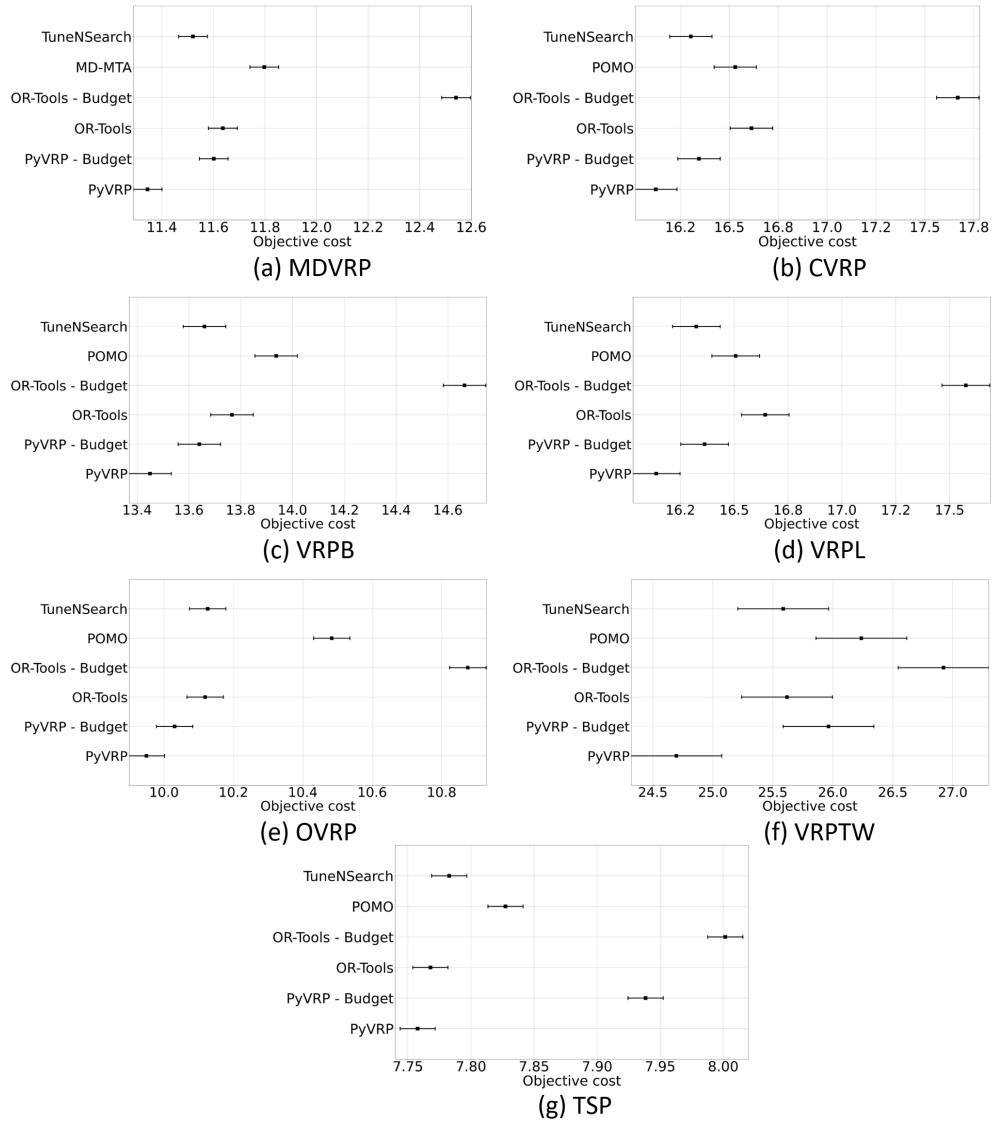


Figure 4: Means plot and 95% confidence level Tukey's HSD intervals for different VRP variants and methods.

### 5.3. Ablation study

To evaluate the impact of the local search algorithm, we conducted an ablation study by varying the number of iterations performed after inference across all VRP variants, as outlined in Table 8. The results reveal that performance sensitivity to the number of iterations varies significantly between tasks. For example, tasks such as VRPTW, VRPB and OVRP demonstrated a higher sensitivity to changes in the number of iterations. In contrast, simpler variants like the CVRP and TSP exhibited much lower sensitivity. We believe this difference may be related to the level of constraints inherent to each task. More constrained tasks likely benefit more from additional iterations, as the search process requires more computational effort to explore the solution space effectively. Overall, we found that 50 iterations offer a good trade-off between solution quality and computational performance for most tasks. Beyond this point, further iterations lead to marginal gains, with the objective function improving at a much slower rate while imposing more



Table 3: Generalization on Cordeau’s benchmark instances (\* represents 0.000 % gap).

Instance	Depots	Customers	BKS	Ours			MD-MTA		
				Obj.	Gap	Time (m)	Obj.	Gap	Time (m)
p01	4	50	577	<b>577</b>	*	0.048	615	6.586 %	0.004
p02	4	50	474	<b>480</b>	<b>1.266</b> %	0.034	517	9.072 %	0.003
p03	5	75	641	<b>649</b>	<b>1.248</b> %	0.049	663	3.432 %	0.003
p04	2	100	1001	<b>1003</b>	<b>0.200</b> %	0.076	1044	4.296 %	0.004
p05	2	100	750	<b>754</b>	<b>0.533</b> %	0.069	785	4.667 %	0.004
p06	3	100	877	<b>888</b>	<b>1.254</b> %	0.071	910	3.763 %	0.004
p07	4	100	882	<b>898</b>	<b>1.814</b> %	0.073	929	5.329 %	0.004
p08	2	249	4372	<b>4493</b>	<b>2.768</b> %	0.283	4773	9.172 %	0.011
p09	3	249	3859	<b>4017</b>	<b>4.094</b> %	0.279	4240	9.873 %	0.012
p10	4	249	3630	<b>3744</b>	<b>3.140</b> %	0.276	4127	13.691 %	0.012
p11	5	249	3545	<b>3632</b>	<b>2.454</b> %	0.272	4034	13.794 %	0.013
p12	2	80	1319	<b>1319</b>	*	0.048	1390	5.383 %	0.003
p13	2	80	1319	<b>1319</b>	*	0.048	1390	5.383 %	0.003
p14	2	80	1360	<b>1360</b>	*	0.050	1390	2.206 %	0.003
p15	4	160	2505	<b>2599</b>	<b>3.752</b> %	0.126	2686	7.225 %	0.006
p16	4	160	2572	<b>2574</b>	<b>0.078</b> %	0.127	2686	4.432 %	0.006
p17	4	160	2709	<b>2709</b>	*	0.127	2728	0.701 %	0.006
p18	6	240	3703	<b>3882</b>	<b>4.834</b> %	0.246	4051	9.398 %	0.013
p19	6	240	3827	<b>3832</b>	<b>0.131</b> %	0.247	4051	5.853 %	0.013
p20	6	240	4058	<b>4069</b>	<b>0.271</b> %	0.245	4096	0.936 %	0.012
p21	9	360	5475	<b>5588</b>	<b>2.064</b> %	0.512	6532	19.306 %	0.039
p22	9	360	5702	<b>5705</b>	<b>0.053</b> %	0.512	6532	14.556 %	0.041
p23	9	360	6079	<b>6129</b>	<b>0.822</b> %	0.519	6532	7.452 %	0.039
Avg. Gap				<b>1.338</b> %			7.239 %		

Table 4: Generalization on VRPL instances, Set-Golden (Golden et al., 1998).

Instance	Customers	Distance Constraint	BKS	Ours			POMO		
				Obj.	Gap	Time (m)	Obj.	Gap	Time (m)
pr01	240	650	5623.5	<b>5782.8</b>	<b>2.833</b> %	0.288	6229.8	10.781 %	0.006
pr02	320	900	8404.6	<b>8539.8</b>	<b>1.609</b> %	0.399	9918.4	18.012 %	0.009
pr03	400	1200	10997.8	<b>11340.5</b>	<b>3.116</b> %	0.622	14067.1	27.908 %	0.013
pr04	480	1600	13588.6	<b>14196.7</b>	<b>4.475</b> %	0.861	17743.7	30.578 %	0.019
pr05	200	1800	6461.0	<b>6582.3</b>	<b>1.877</b> %	0.183	7816.9	20.986 %	0.006
pr06	280	1500	8400.3	<b>8597.6</b>	<b>2.349</b> %	0.313	10290.7	22.504 %	0.008
pr07	360	1300	10102.7	<b>10336.8</b>	<b>2.317</b> %	0.539	12941.7	28.101 %	0.011
pr08	440	1200	11635.3	<b>12042.8</b>	<b>3.502</b> %	0.767	16006.8	37.571 %	0.016
Avg. Gap				<b>2.760</b> %			24.555 %		

computational time. Extending the local search for too many iterations would diminish the computational efficiency enabled by the reinforcement learning component, which goes against the intended purpose of our method.

#### 5.4. Why pre-train on the MDVRP?

We argue that one of the main contributions of this paper is that pre-training the model on the MDVRP can lead to a better generalization across different single- and multi-depot tasks. To assess the effectiveness of pre-training the model on MDVRP data, we compared TuneNSearch with a model pre-trained on the CVRP. We evaluate both models on their zero-shot generalization performance to both single-depot and multi-depot variants. For the multi-depot variants, we incorporated the constraints outlined in Section 3.3 into the classic MDVRP, resulting in the following variants: MDVRP with backhauls (MDVRPB), MDVRP

Table 5: Generalization on CVRPLIB instances, Set-X (Uchoa et al., 2017).

Instance	BKS	POMO		AMDKD-POMO		Meta-POMO		Omni-POMO		Ours	
		Obj.	Gap	Obj.	Gap	Obj.	Gap	Obj.	Gap	Obj.	Gap
X-n101-k25	27591	28804	4.396 %	28947	4.915 %	29647	7.452 %	29442	6.709 %	<b>28157</b>	<b>2.051 %</b>
X-n153-k22	21220	23701	11.692 %	23179	9.232 %	23428	10.405 %	22810	7.493 %	<b>21400</b>	<b>0.848 %</b>
X-n200-k36	58578	60983	4.106 %	61074	4.261 %	61632	5.214 %	61496	4.981 %	<b>59322</b>	<b>1.270 %</b>
X-n251-k28	38684	40027	3.472 %	40262	4.079 %	40477	4.635 %	40059	3.554 %	<b>39617</b>	<b>2.412 %</b>
X-n303-k21	21736	22724	4.545 %	22861	5.176 %	22661	4.256 %	22624	4.085 %	<b>22271</b>	<b>2.461 %</b>
X-n351-k40	25896	27410	5.846 %	27431	5.928 %	27992	8.094 %	27515	6.252 %	<b>26899</b>	<b>3.873 %</b>
X-n401-k29	66154	68435	3.448 %	68579	3.666 %	68272	3.202 %	68234	3.144 %	<b>67406</b>	<b>1.892 %</b>
X-n459-k26	24139	26612	10.245 %	26255	8.766 %	25789	6.835 %	25706	6.492 %	<b>25207</b>	<b>4.424 %</b>
X-n502-k39	69226	71435	3.191 %	71390	3.126 %	71209	2.864 %	70769	2.229 %	<b>69780</b>	<b>0.800 %</b>
X-n548-k50	86700	90904	4.849 %	90890	4.833 %	90743	4.663 %	90592	4.489 %	<b>88400</b>	<b>1.961 %</b>
X-n599-k92	108451	115894	6.863 %	115702	6.686 %	115627	6.617 %	116964	7.850 %	<b>111898</b>	<b>3.178 %</b>
X-n655-k131	106780	110327	3.322 %	111587	4.502 %	110756	3.723 %	110096	3.105 %	<b>107637</b>	<b>0.803 %</b>
X-n701-k44	81923	86933	6.115 %	88166	7.621 %	86605	5.715 %	86005	4.983 %	<b>84894</b>	<b>3.627 %</b>
X-n749-k98	77269	83294	7.797 %	83934	8.626 %	84406	9.237 %	83893	8.573 %	<b>80278</b>	<b>3.894 %</b>
X-n801-k40	73311	80584	9.921 %	80897	10.348 %	79077	7.865 %	78171	6.630 %	<b>75870</b>	<b>3.491 %</b>
X-n856-k95	88965	96398	8.355 %	95809	7.693 %	95801	7.684 %	96739	8.748 %	<b>90418</b>	<b>1.633 %</b>
X-n895-k37	53860	61604	14.378 %	62316	15.700 %	59778	10.988 %	58947	9.445 %	<b>56456</b>	<b>4.820 %</b>
X-n957-k87	85465	93221	9.075 %	93995	9.981 %	92647	8.403 %	92011	7.659 %	<b>87563</b>	<b>2.455 %</b>
X-n1001-k43	72355	82046	13.394 %	82855	14.512 %	79347	9.663 %	78955	9.122 %	<b>76447</b>	<b>5.655 %</b>
Avg. Gap		7.106 %		7.353 %		6.711 %		6.081 %		<b>2.713 %</b>	

Table 6: Generalization on TSPLIB instances (Reinelt, 1991).

Instance	BKS	POMO		AMDKD-POMO		Meta-POMO		Omni-POMO		Ours	
		Obj.	Gap	Obj.	Gap	Obj.	Gap	Obj.	Gap	Obj.	Gap
kroA100	21282	<b>21282</b>	*	21360	0.366 %	21308	0.122 %	21305	0.108 %	21306	0.113 %
kroA150	26524	<b>26823</b>	<b>1.127 %</b>	26997	1.783 %	26852	1.237 %	26873	1.316 %	26875	1.323 %
kroA200	29368	<b>29745</b>	<b>1.284 %</b>	30196	2.819 %	29749	1.297 %	29823	1.549 %	29770	1.369 %
kroB200	29437	30060	2.116 %	30188	2.551 %	29896	1.559 %	29814	1.281 %	<b>29800</b>	<b>1.233 %</b>
ts225	126643	131208	3.605 %	128210	1.237 %	131877	4.133 %	128770	1.679 %	<b>127763</b>	<b>0.884 %</b>
tsp225	3916	4040	3.166 %	4074	4.035 %	4047	3.345 %	4008	2.349 %	<b>3976</b>	<b>1.532 %</b>
pr226	80369	81509	1.418 %	82430	2.564 %	81968	1.990 %	81839	1.829 %	<b>80735</b>	<b>0.455 %</b>
pr264	49135	50513	2.804 %	51656	5.131 %	50065	1.893 %	50649	3.081 %	<b>49653</b>	<b>1.054 %</b>
a280	2579	2714	5.234 %	2773	7.522 %	2703	4.808 %	2695	4.498 %	<b>2632</b>	<b>2.055 %</b>
pr299	48191	50571	4.939 %	51270	6.389 %	49773	3.283 %	49348	2.401 %	<b>48833</b>	<b>1.332 %</b>
lin318	42029	44011	4.716 %	44154	5.056 %	43807	4.230 %	43828	4.280 %	<b>43022</b>	<b>2.363 %</b>
rd400	15281	16254	6.367 %	16610	8.697 %	16153	5.706 %	15948	4.365 %	<b>15794</b>	<b>3.357 %</b>
fl417	11861	12940	9.097 %	13129	10.690 %	12849	8.330 %	12683	6.930 %	<b>11944</b>	<b>0.700 %</b>
pr439	107217	115651	7.866 %	117872	9.938 %	114872	7.140 %	114487	6.781 %	<b>111502</b>	<b>3.997 %</b>
pcb442	50778	55273	8.852 %	56225	10.727 %	55507	9.313 %	54531	7.391 %	<b>52635</b>	<b>3.657 %</b>
d493	35002	38388	9.674 %	38400	9.708 %	38641	10.396 %	38169	9.048 %	<b>36975</b>	<b>5.637 %</b>
u574	36905	41574	12.651 %	41426	12.250 %	41418	12.229 %	40515	9.782 %	<b>38918</b>	<b>5.454 %</b>
rat575	6773	7617	12.461 %	7707	13.790 %	7620	12.505 %	7658	13.067 %	<b>7197</b>	<b>6.260 %</b>
p654	34643	38556	11.295 %	39327	13.521 %	38307	10.576 %	37488	8.212 %	<b>35265</b>	<b>1.795 %</b>
d657	48912	55133	12.719 %	55143	12.739 %	54715	11.864 %	54346	11.110 %	<b>51510</b>	<b>5.312 %</b>
u724	41910	48855	16.571 %	48738	16.292 %	48272	15.180 %	48026	14.593 %	<b>43886</b>	<b>4.715 %</b>
rat783	8806	10401	18.113 %	10338	17.397 %	10228	16.148 %	10300	16.966 %	<b>9409</b>	<b>6.848 %</b>
pr1002	259045	310855	20.000 %	312299	20.558 %	308281	19.007 %	305777	18.040 %	<b>278844</b>	<b>7.643 %</b>
Avg. Gap		7.264 %		8.511 %		7.230 %		6.550 %		<b>3.004 %</b>	

with duration limits (MDVRPL), MDVRP with open routes (MDOVRP), and MDVRP with time windows (MDVRPTW).

Like TuneNSearch, we also pre-trained the CVRP model for 100 epochs, using the same deep neural network architecture. Table 9 presents the inference results for both models in terms of the objective value and the performance gap between TuneNSearch and the CVRP pre-trained model. The evaluation was conducted on 1280 randomly generated instances for each VRP variant. In both cases, inference was performed greedily with instance augmentation. In these experiments, we did not apply the local search

Table 7: Generalization on VRPTW instances, Set-Solomon (Solomon, 1987).

Instance	BKS	POMO		POMO-MTL		MVMoE/4E		MVMoE/4E-L		Ours	
		Obj.	Gap	Obj.	Gap	Obj.	Gap	Obj.	Gap	Obj.	Gap
R101	1637.7	1805.6	10.252 %	1821.2	11.205 %	1798.1	9.794 %	1730.1	5.641 %	<b>1644.2</b>	<b>0.400 %</b>
R102	1466.6	1556.7	6.143 %	1596.0	8.823 %	1572.0	7.187 %	1574.3	7.345 %	<b>1493.7</b>	<b>1.848 %</b>
R103	1208.7	1341.4	10.979 %	1327.3	9.812 %	1328.2	9.887 %	1359.4	12.470 %	<b>1223.5</b>	<b>1.224 %</b>
R104	971.5	1118.6	15.142 %	1120.7	15.358 %	1124.8	15.780 %	1098.8	13.100 %	<b>977.8</b>	<b>0.648 %</b>
R105	1355.3	1506.4	11.149 %	1514.6	11.754 %	1479.4	9.157 %	1456.0	7.433 %	<b>1364.5</b>	<b>0.679 %</b>
R106	1234.6	1365.2	10.578 %	1380.5	11.818 %	1362.4	10.352 %	1353.5	9.627 %	<b>1249.6</b>	<b>1.215 %</b>
R107	1064.6	1214.2	14.052 %	1209.3	13.592 %	1181.1	11.037 %	1196.5	12.391 %	<b>1099.3</b>	<b>3.259 %</b>
R108	932.1	1058.9	13.604 %	1061.8	13.915 %	1023.2	9.774 %	1039.1	11.481 %	<b>961.2</b>	<b>3.122 %</b>
R109	1146.9	1249.0	8.902 %	1265.7	10.358 %	1255.6	9.478 %	1224.3	6.750 %	<b>1158.5</b>	<b>1.011 %</b>
R110	1068.0	1180.4	10.524 %	1171.4	9.682 %	1185.7	11.021 %	1160.2	8.635 %	<b>1087.9</b>	<b>1.863 %</b>
R111	1048.7	1177.2	12.253 %	1211.5	15.524 %	1176.1	12.148 %	1197.8	14.220 %	<b>1060.1</b>	<b>1.087 %</b>
R112	948.6	1063.1	12.070 %	1057.0	11.427 %	1045.2	10.183 %	1044.2	10.082 %	<b>961.8</b>	<b>1.391 %</b>
RC101	1619.8	2643.0	63.168 %	1833.3	13.181 %	1774.4	9.544 %	1749.2	7.988 %	<b>1639.8</b>	<b>1.235 %</b>
RC102	1457.4	1534.8	5.311 %	1546.1	6.086 %	1544.5	5.976 %	1556.1	6.771 %	<b>1477.2</b>	<b>1.359 %</b>
RC103	1258.0	1407.5	11.884 %	1396.2	10.986 %	1402.5	11.486 %	1415.3	12.502 %	<b>1279.1</b>	<b>1.677 %</b>
RC104	1132.3	1261.8	11.437 %	1271.7	12.311 %	1265.4	11.755 %	1264.2	11.649 %	<b>1163.4</b>	<b>2.747 %</b>
RC105	1513.7	1612.9	6.553 %	1644.9	8.668 %	1635.5	8.047 %	1619.4	6.980 %	<b>1549.2</b>	<b>2.345 %</b>
RC106	1372.7	1539.3	12.137 %	1552.8	13.120 %	1505.0	9.638 %	1509.5	9.968 %	<b>1391.0</b>	<b>1.333 %</b>
RC107	1207.8	1347.7	11.583 %	1384.8	14.655 %	1351.6	11.906 %	1324.1	9.625 %	<b>1214.9</b>	<b>0.588 %</b>
RC108	1114.2	1305.5	17.169 %	1274.4	14.378 %	1254.2	12.565 %	1247.2	11.939 %	<b>1134.3</b>	<b>1.804 %</b>
RC201	1261.8	2045.6	62.118 %	1761.1	39.570 %	1577.3	25.004 %	1517.8	20.285 %	<b>1280.9</b>	<b>1.514 %</b>
RC202	1092.3	1805.1	65.257 %	1486.2	36.062 %	1616.5	47.990 %	1480.3	35.520 %	<b>1106.6</b>	<b>1.309 %</b>
RC203	923.7	1470.4	59.186 %	1360.4	47.277 %	1473.5	59.521 %	1479.6	60.182 %	<b>940.4</b>	<b>1.808 %</b>
RC204	783.5	1323.9	68.973 %	1331.7	69.968 %	1286.6	64.212 %	1232.8	57.342 %	<b>791.4</b>	<b>1.008 %</b>
RC205	1154.0	1568.4	35.910 %	1539.2	33.380 %	1537.7	33.250 %	1440.8	24.850 %	<b>1171.1</b>	<b>1.482 %</b>
RC206	1051.1	1707.5	62.449 %	1472.6	40.101 %	1468.9	39.749 %	1394.5	32.671 %	<b>1086.3</b>	<b>3.349 %</b>
RC207	962.9	1567.2	62.758 %	1375.7	42.870 %	1442.0	49.756 %	1346.4	39.831 %	<b>981.9</b>	<b>1.973 %</b>
RC208	776.1	1505.4	93.970 %	1185.6	52.764 %	1107.4	42.688 %	1167.5	50.437 %	<b>782.2</b>	<b>0.786 %</b>
Avg. Gap		28.054 %		21.380 %		20.317 %		18.490 %		<b>1.574 %</b>	

algorithm.

Results show that TuneNSearch performs just as well as the CVRP pre-trained model on single-depot variants, with a negligible performance gap between both methods. However, on multi-depot variants, TuneNSearch performs significantly better on all instance sizes. The performance gap becomes especially more pronounced as problem size increases: while the CVRP pre-trained model performs reasonably well on small instances (with 20 nodes), its performance degrades sharply on larger problems.

### 5.5. Impact of integrating the residual E-GAT with POMO

Another key contribution of our work is the integration of POMO (Kwon et al., 2020) with the residual E-GAT encoder (Lei et al., 2022). The residual E-GAT, originally built on top of the attention model (Kool et al., 2019), improves the learning process by incorporating edge information and adding residual connections between layers. This allows the model to capture richer contextual information about the problem, resulting in more accurate attention coefficient computations. When combined with POMO, this improved encoding can lead to a better utilization of POMO’s multiple starting nodes, generating higher quality solutions. However, the impact of the residual E-GAT has not previously been evaluated in conjunction with POMO — a framework that has already demonstrated superior performance compared to the original attention model.

In this subsection, we compare the performance of TuneNSearch with both the original POMO and residual E-GAT models. Our aim is to analyze how effective the encoding capability of each approach is, and how well they capture the graph features of the VRP. We begin by examining the training patterns of all three approaches, analyzing the evolution of the average objective function at each epoch, illustrated in Fig. 5. The models were trained in MDVRP instances with 20, 50 and 100 customers and 2, 3 and 4 depots, respectively. Across all three problem sizes, TuneNSearch exhibited a more efficient convergence. In

Table 8: Ablation study on the number of local search iterations on 1280 randomly generated instances.

Number of iterations	Problem	$n = 20$		$n = 50$		$n = 100$	
		Obj.	Time (m)	Obj.	Time (m)	Obj.	Time (m)
5	MDVRP	4.498	0.124	7.616	0.282	11.669	0.929
	CVRP	4.969	0.129	9.481	0.252	16.368	0.793
	VRPB	4.599	0.119	8.460	0.257	14.304	0.767
	VRPL	4.991	0.123	9.481	0.259	16.378	0.828
	OVRP	3.485	0.124	6.236	0.239	10.251	0.791
	VRPTW	7.684	0.134	14.910	0.310	25.683	0.975
	TSP	3.831	0.119	5.713	0.211	7.833	0.599
	Average	4.865	0.125	8.842	0.259	14.641	0.812
10	MDVRP	4.493	0.143	7.594	0.365	11.646	1.107
	CVRP	4.965	0.144	9.465	0.331	16.357	1.055
	VRPB	4.596	0.126	8.436	0.328	14.288	1.097
	VRPL	4.987	0.147	9.464	0.332	16.366	1.063
	OVRP	3.482	0.149	6.215	0.318	10.217	0.999
	VRPTW	7.654	0.148	14.792	0.427	25.518	1.296
	TSP	3.831	0.129	5.712	0.253	7.830	0.784
	Average	4.858	0.141	8.811	0.336	14.603	1.057
25	MDVRP	4.487	0.191	7.563	0.584	11.606	1.793
	CVRP	4.963	0.153	9.441	0.555	16.332	1.763
	VRPB	4.593	0.155	8.402	0.559	14.249	1.847
	VRPL	4.984	0.162	9.443	0.570	16.338	1.804
	OVRP	3.479	0.143	6.188	0.514	10.167	1.657
	VRPTW	7.624	0.181	14.667	0.763	25.320	2.286
	TSP	3.830	0.153	5.708	0.413	7.823	1.302
	Average	4.851	0.163	8.773	0.565	14.548	1.779
50	MDVRP	4.486	0.251	7.541	0.938	11.570	2.902
	CVRP	4.962	0.214	9.425	0.936	16.306	2.975
	VRPB	4.592	0.228	8.382	0.963	14.212	2.945
	VRPL	4.983	0.222	9.427	0.994	14.313	3.048
	OVRP	3.478	0.200	6.173	0.866	10.125	2.746
	VRPTW	7.610	0.274	14.592	1.394	25.178	4.027
	TSP	3.830	0.168	5.705	0.676	7.816	2.190
	Average	4.849	0.222	8.749	0.967	14.217	2.976
100	MDVRP	4.485	0.371	7.525	1.652	11.526	5.128
	CVRP	4.962	0.349	9.410	1.711	16.278	5.396
	VRPB	4.592	0.347	8.365	1.705	14.170	5.446
	VRPL	4.983	0.354	9.412	1.771	16.282	5.460
	OVRP	3.478	0.326	6.162	1.549	10.084	4.917
	VRPTW	7.604	0.463	14.539	2.622	25.026	7.258
	TSP	3.830	0.249	5.704	1.229	7.808	4.079
	Average	4.848	0.351	8.731	1.748	14.453	5.383

comparison to the residual E-GAT model, the gap was a lot more noticeable, since it does not incorporate the exploitation of solutions symmetries and multiple starting nodes introduced by POMO.

In Table 10, we compared the inference results of all three methods. The evaluation was performed on 1280 randomly generated instances, using a greedy decoding. Both POMO and TuneNSearch utilized instance augmentation, with no local search performed after inference. We note that the residual E-GAT model did not use instance augmentation, as it does not exploit solution symmetries.

The results show that TuneNSearch outperforms the other methods in all problem sizes. These findings confirm that integrating the residual E-GAT with POMO improves learning performance, enabling a more effective encoding of the problem’s features.

Table 9: Zero-shot generalization comparison on 1280 randomly generated instances: Pre-training on MDVRP vs. CVRP.

Method		$n = 20$		$n = 50$		$n = 100$	
		Obj.	Performance gap	Obj.	Performance gap	Obj.	Performance gap
VRPB	Ours	4.665		8.752		15.040	
	CVRP pre-trained	<b>4.657</b>	0.172 %	<b>8.714</b>	0.436 %	<b>15.007</b>	0.220 %
VRPL	Ours	5.036		9.550		16.597	
	CVRP pre-trained	<b>5.025</b>	0.219 %	<b>9.496</b>	0.569 %	<b>16.509</b>	0.533 %
OVRP	Ours	<b>3.879</b>		7.257		12.223	
	CVRP pre-trained	3.902	-0.589 %	<b>7.246</b>	0.152 %	<b>12.130</b>	0.767 %
VRPTW	Ours	<b>8.652</b>		18.340		<b>31.468</b>	
	CVRP pre-trained	8.746	-1.075 %	<b>18.129</b>	1.164 %	31.687	-0.691 %
Average (Single-depot)	Ours	<b>5.558</b>		10.975		<b>18.832</b>	
	CVRP pre-trained	5.582	-0.430 %	<b>10.896</b>	0.725 %	18.833	-0.005 %
MDVRPB	Ours	<b>4.343</b>		<b>7.203</b>		<b>11.003</b>	
	CVRP pre-trained	4.907	-11.494 %	9.293	-22.490 %	21.801	-49.530 %
MDVRPL	Ours	<b>4.462</b>		<b>7.514</b>		<b>11.540</b>	
	CVRP pre-trained	5.023	-11.169 %	9.720	-22.695 %	21.609	-46.596 %
MDOVRP	Ours	<b>3.613</b>		<b>6.046</b>		<b>9.253</b>	
	CVRP pre-trained	3.949	-8.508 %	7.584	-20.279 %	15.556	-40.518 %
MDVRPTW	Ours	<b>8.795</b>		<b>17.054</b>		<b>27.310</b>	
	CVRP pre-trained	10.107	-12.981 %	21.936	-22.256 %	47.922	-43.012 %
Average (Multi-depot)	Ours	<b>5.303</b>		<b>9.454</b>		<b>14.776</b>	
	CVRP pre-trained	5.996	-11.558 %	12.133	-22.080 %	26.722	-44.705 %

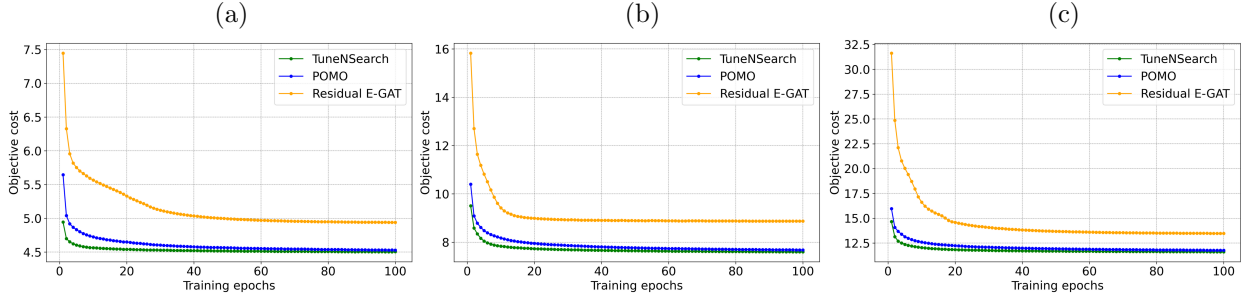

 Figure 5: MDVRP training curves of POMO, Residual E-GAT, and TuneNSearch - (a)  $n = 20$ ; (b)  $n = 50$ ; (c)  $n = 100$ .

Table 10: Average inference results on 1280 randomly generated MDVRP instances: impact of integrating the residual E-GAT with POMO.

Method	$n = 20$		$n = 50$		$n = 100$	
	Obj.	Time (m)	Obj.	Time (m)	Obj.	Time (m)
Ours	<b>4.526</b>	0.052	<b>7.647</b>	0.135	<b>11.734</b>	0.501
POMO	4.537	0.040	7.691	0.084	11.840	0.291
Residual E-GAT	4.941	0.065	10.585	0.080	13.130	0.116

### 5.6. Analysis of the fine-tuning phase

Besides evaluating the performance during inference, we also compare the training patterns of POMO and TuneNSearch (only the fine-tuned models, excluding the MDVRP), averaged across all VRP variants (see Fig. 6). Since POMO was trained for 100 epochs while TuneNSearch underwent fine-tuning for 20 epochs, we normalized the training progress, presenting it as a percentage rather than using the number of epochs.

For instances with 20 customers, POMO slightly outperforms TuneNSearch towards the end of training, however, for problems with 50 and 100 customers, POMO is inferior to TuneNSearch. Notably, the efficiency of our method is particularly evident at the beginning of training, since it benefits from prior knowledge



gained during the pre-training phase. Furthermore, the performance gap between TuneNSearch and POMO appears to widen as problem sizes increase.

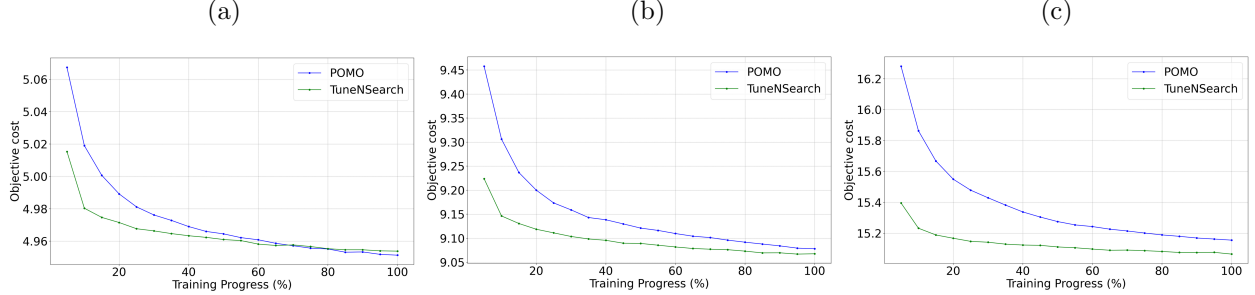


Figure 6: Training curves of POMO and TuneNSearch - (a)  $n = 20$ ; (b)  $n = 50$ ; (c)  $n = 100$ .

Moreover, Table 11 presents the average training times for all models considered in this study. We note that the results of POMO and TuneNSearch are aggregated across all VRP variants. As shown, TuneNSearch requires about one-third of the computational time needed to train POMO from the beginning for each variant. It is important to highlight that the pre-trained MDVRP model incurs higher training time than POMO due to its use of a hidden dimension of  $h_x = 256$  instead of 128. Nonetheless, the strength of TuneNSearch lies in its capability to solve multiple VRP variants with the same pre-trained model and a fast fine-tuning phase.

Table 11: Average training time (m) for all models.

	$n = 20$	$n = 50$	$n = 100$
MD-MTA	507.52	1690.24	3525.12
POMO	144.88	578.29	1280.45
Ours (pre-trained MDVRP)	243.07	1119.33	2207.62
Ours (fine-tuning)	47.96	192.08	391.91

### 5.7. Computational runtime complexity

Next, we investigate the computational runtime complexity of TuneNSearch on a set of benchmark instances, which are significantly large — up to 1000 nodes. The primary goal of this analysis is to understand how the integration of the local search algorithm scales with increasing problem sizes.

The experimental results, presented in Fig. 7, reveal that TuneNSearch exhibits polynomial runtime growth with respect to instance size (defined as a function of the number of nodes). More specifically, the trend follows a quadratic pattern, as indicated by the fitted curve equation of  $y = 0.0007x^2 - 0.2546x + 33.3775$ , with an  $R^2$  value of 0.9798. While this scaling behavior is encouraging, especially compared to traditional methods, which typically present an exponential complexity, there is still room for improvement in computational efficiency. One such opportunity lies in reducing the number of starting nodes used by the decoder. Our decoder generates multiple candidate solutions per instance by initializing from every possible node. Although this approach may improve solution quality, it increases the computational runtime. To address this, we reevaluated TuneNSearch on all benchmark problems while limiting the maximum number of starting nodes to 200. The results show that this adjustment leads to a substantial reduction in runtime, particularly for larger instances. With this modification, the runtime still follows a polynomial trend, but with a more favorable curve equation of  $y = 0.0002x^2 + 0.0119x + 0.2375$ , and an improved  $R^2$  value of 0.9849. Furthermore, reducing the number of starting nodes to 200 had a negligible impact on the algorithm’s effectiveness, with the average solution quality deteriorating by less than 1%.

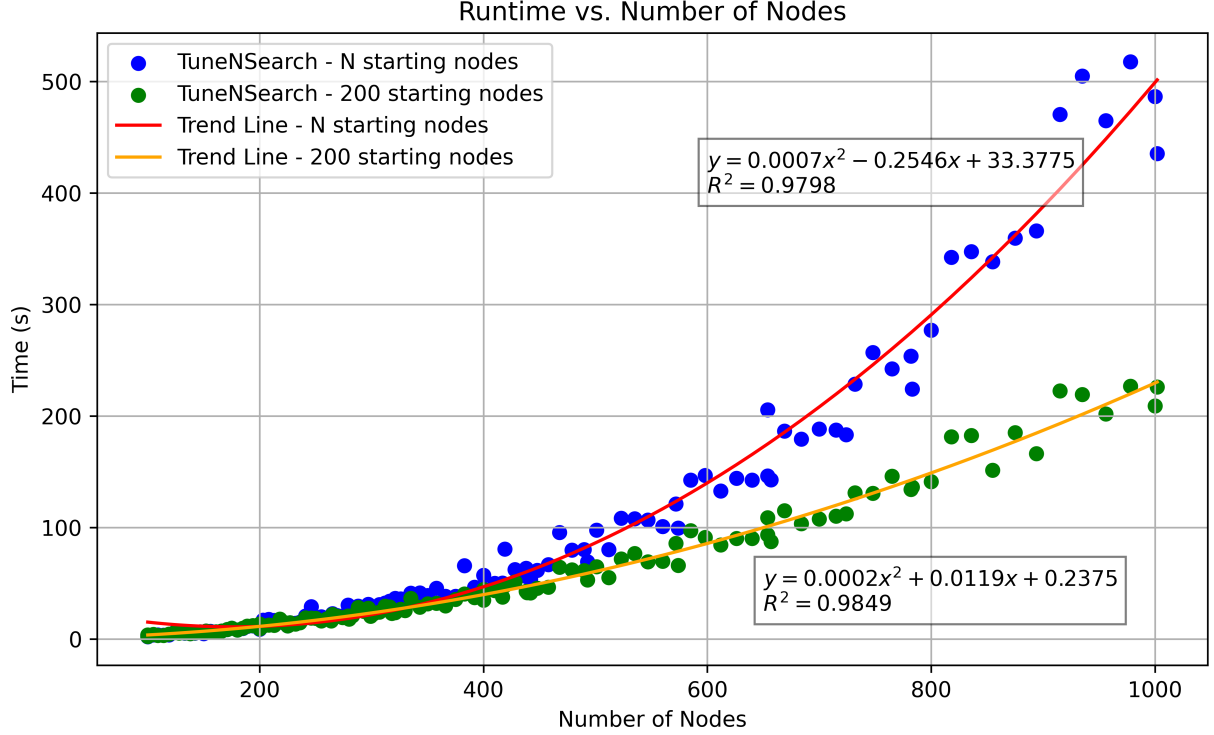


Figure 7: TuneNSearch computational runtime on varying instance sizes.

## 6. Conclusion

In this paper, we introduce TuneNSearch, a novel transfer learning method designed for adaptation to various VRP variants through an efficient fine-tuning phase. Our approach builds on the model architecture of [Kwon et al. \(2021\)](#) by enhancing the encoder with a residual E-GAT. While [Lei et al. \(2022\)](#) previously integrated this technique into the attention model ([Kool et al., 2019](#)), we extend its application to POMO, demonstrating that this extension improves the model’s ability to encode the problem’s features more effectively. Then, we pre-trained our model using MDVRP data, exploiting its complex graph-structured features. This strategy allows for a broader generalization across a variety of VRP variants, including both single- and multi-depot tasks. To evaluate the effectiveness of our approach, we compared it to an identical model pre-trained on the CVRP. The results demonstrate that while both methods perform similarly on single-depot variants, TuneNSearch substantially outperforms the CVRP-pre-trained model on multi-depot variants. To validate the learning process on the MDVRP, we compared TuneNSearch with MD-MTA, demonstrating superior results across all problem sizes while requiring much less training time. Finally, we integrated an efficient local search method to refine the quality of solutions generated by our model, leading to significant performance improvements with a small computational overhead. We also conducted an ablation study to assess the impact of varying the number of local search iterations. Our findings indicate that more constrained tasks tend to benefit more from this procedure.

To evaluate the generalization of TuneNSearch, we performed extensive experiments on numerous VRP variants and baselines. Experimental results on randomly generated instances show that TuneNSearch outperforms POMO, which is specialized for each variant, while requiring only one-fifth of the total training epochs. Moreover, TuneNSearch achieves performance comparable to OR-Tools guided local search procedure, often even outperforming it on many occasions, delivering results at a fraction of the computational

time. We also provide results on benchmark instances of different VRP variants, where TuneNSearch outperforms other state-of-the-art neural-based models on most problems, narrowing the existing solution gaps. These findings demonstrate not only TuneNSearch’s strong cross-task generalization, but also its cross-size and cross-distribution generalization.

In addition to these results, we believe TuneNSearch holds significant potential for solving real-world problems. Many industries frequently face large, complex problems that demand rapid and near-optimal solutions. Traditional optimization algorithms struggle to generate high-quality solutions within polynomial time due to the NP-hard nature of routing problems, while conventional heuristics often result in large integrality gaps. TuneNSearch addresses these challenges by delivering good performance across various VRP variants while maintaining computational efficiency.

### 6.1. Limitations and future work

While this study offers insights into the development of generalizable neural-based methods, there are certain limitations to our approach. First, TuneNSearch is specifically designed to solve traditional VRPs, with the constraints outlined in Section 3.3 (or any combination of such constraints). Although it is possible to extend our method to other problems, such as the orienteering problem or prize collecting TSP, doing so would require manual adjustments to the Transformer architecture to accommodate new constraints. Second, TuneNSearch assumes that the objective function — minimizing the total distance traveled — remains unchanged across all scenarios. Modifying the objective during the fine-tuning phase may impact the learning process, as the neurons of the pre-trained model are already optimized for distance minimization. As such, in these scenarios, it is likely that TuneNSearch would require a higher number of fine-tuning epochs.

Looking ahead, we aim to extend TuneNSearch beyond traditional VRP variants to address a broader range of combinatorial problems. In particular, we plan to adapt our method to scheduling problems, which can be framed as variations of the TSP. Another promising direction is to further enhance the performance of TuneNSearch to reduce the integrality gaps even further. One possible approach could involve clustering training instances based on their underlying distributions and training specialized local models for each subset, which could potentially improve generalization. Alternatively, integrating decomposition approaches with learning-based methods to solve the VRP in a “divide-and-conquer” manner is another promising research direction.

## Acknowledgements

This work has been supported by the European Union under the Next Generation EU, through a grant of the Portuguese Republic’s Recovery and Resilience Plan Partnership Agreement [project C645808870-00000067], within the scope of the project PRODUTECH R3 – “Agenda Mobilizadora da Fileira das Tecnologias de Produção para a Reindustrialização”, Total project investment: 166.988.013,71 Euros; Total Grant: 97.111.730,27 Euros; and by the European Regional Development Fund (ERDF) through the Operational Program for Competitiveness and Internationalization (COMPETE 2020) under the project POCI-01-0247-FEDER-046102 (PRODUTECH4S&C); and by national funds through FCT – Fundação para a Ciência e a Tecnologia, under projects UID/00285 - Centre for Mechanical Engineering, Materials and Processes and LA/P/0112/2020.

## References

- Baldacci, R., Mingozzi, A., Roberti, R., 2012. Recent exact algorithms for solving the vehicle routing problem under capacity and time window constraints. *European Journal of Operational Research* 218, 1–6. URL: <https://www.sciencedirect.com/science/article/pii/S0377221711006692>, doi:10.1016/j.ejor.2011.07.037.
- Bello, I., Pham, H., Le, Q.V., Norouzi, M., Bengio, S., 2017. Neural combinatorial optimization with reinforcement learning, in: 5th International Conference on Learning Representations, ICLR 2017 - Workshop Track Proceedings.
- Bengio, Y., Lodi, A., Prouvost, A., 2021. Machine learning for combinatorial optimization: A methodological tour d’horizon. *European Journal of Operational Research* 290, 405–421. URL: <https://www.sciencedirect.com/science/article/pii/S0377221720306895>, doi:10.1016/j.ejor.2020.07.063.

- Berto, F., Hua, C., Zepeda, N.G., Hottung, A., Wouda, N., Lan, L., Park, J., Tierney, K., Park, J., 2025. Routefinder: Towards foundation models for vehicle routing problems. arXiv abs/2406.15007.
- Bi, J., Ma, Y., Wang, J., Cao, Z., Chen, J., Sun, Y., Chee, Y.M., 2022. Learning generalizable models for vehicle routing problems via knowledge distillation, in: *Advances in Neural Information Processing Systems*.
- Bi, J., Ma, Y., Zhou, J., Song, W., Cao, Z., Wu, Y., Zhang, J., 2025. Learning to handle complex constraints for vehicle routing problems, in: *Advances in Neural Information Processing Systems*.
- Braekers, K., Ramaekers, K., Nieuwenhuyse, I.V., 2016. The vehicle routing problem: State of the art classification and review. *Computers & Industrial Engineering* 99, 300–313. URL: <https://www.sciencedirect.com/science/article/pii/S0360835215004775>, doi:10.1016/j.cie.2015.12.007.
- Cattaruzza, D., Absi, N., Feillet, D., González-Feliu, J., 2017. Vehicle routing problems for city logistics. *EURO Journal on Transportation and Logistics* 6, 51–79. doi:10.1007/s13676-014-0074-0.
- Chalumeau, F., Surana, S., Bonnet, C., Grinsztajn, N., Pretorius, A., Laterre, A., Barrett, T.D., 2023. Combinatorial optimization with policy adaptation using latent space search, in: *Advances in Neural Information Processing Systems*.
- Chao, I.M., Golden, B.L., Wasil, E., 1993. A new heuristic for the multi-depot vehicle routing problem that improves upon best-known solutions. *American Journal of Mathematical and Management Sciences* 13, 371–406. URL: <https://doi.org/10.1080/01966324.1993.10737363>, doi:10.1080/01966324.1993.10737363. doi: 10.1080/01966324.1993.10737363.
- Chen, X., Tian, Y., 2019. Learning to perform local rewriting for combinatorial optimization, in: *Advances in Neural Information Processing Systems*.
- Christofides, N., Eilon, S., 1969. An algorithm for the vehicle-dispatching problem. *Journal of the Operational Research Society* 20, 309–318. URL: <https://doi.org/10.1057/jors.1969.75>, doi:10.1057/jors.1969.75.
- Cordeau, J.F., Gendreau, M., Laporte, G., 1997. A tabu search heuristic for periodic and multi-depot vehicle routing problems. *Networks* 30, 105–119. doi:10.1002/(SICI)1097-0037(199709)30:2<105::AID-NET5>3.0.CO;2-G.
- Dong, L., Yang, N., Wang, W., Wei, F., Liu, X., Wang, Y., Gao, J., Zhou, M., Hon, H.W., 2019. Unified language model pre-training for natural language understanding and generation, in: *Advances in Neural Information Processing Systems*.
- Elatar, S., Abouelmehdi, K., Riffi, M.E., 2023. The vehicle routing problem in the last decade: variants, taxonomy and metaheuristics. *Procedia Computer Science* 220, 398–404. URL: <https://www.sciencedirect.com/science/article/pii/S1877050923005860>, doi:10.1016/j.procs.2023.03.051. the 14th International Conference on Ambient Systems, Networks and Technologies Networks (ANT) and The 6th International Conference on Emerging Data and Industry 4.0 (EDI40).
- Fitzpatrick, J., Ajwani, D., Carroll, P., 2024. A scalable learning approach for the capacitated vehicle routing problem. *Computers & Operations Research* 171, 106787. URL: <https://www.sciencedirect.com/science/article/pii/S0305054824002594>, doi:10.1016/j.cor.2024.106787.
- Furnon, V., Perron, L., 2024. Or-tools routing library. URL: <https://developers.google.com/optimization/routing/>.
- Gillett, B.E., Johnson, J.G., 1976. Multi-terminal vehicle-dispatch algorithm. *Omega* 4, 711–718. URL: <https://www.sciencedirect.com/science/article/pii/S0305048376900979>, doi:10.1016/0305-0483(76)90097-9.
- Golden, B.L., Wasil, E.A., Kelly, J.P., Chao, I.M., 1998. The Impact of Metaheuristics on Solving the Vehicle Routing Problem: Algorithms, Problem Sets, and Computational Results. Springer US. pp. 33–56. URL: [https://doi.org/10.1007/978-1-4615-5755-5\\_2](https://doi.org/10.1007/978-1-4615-5755-5_2), doi:10.1007/978-1-4615-5755-5\_2.
- Grinsztajn, N., Furelos-Blanco, D., Surana, S., Bonnet, C., Barrett, T.D., 2023. Winner takes it all: Training performant rl populations for combinatorial optimization, in: *Advances in Neural Information Processing Systems*.
- Helsgaun, K., 2000. An effective implementation of the lin-kernighan traveling salesman heuristic. *European Journal of Operational Research* 126, 106–130. URL: <https://www.sciencedirect.com/science/article/pii/S0377221799002842>, doi:10.1016/S0377-2217(99)00284-2.
- Helsgaun, K., 2017. An extension of the lin-kernighan-helsgaun tsp solver for constrained traveling salesman and vehicle routing problems. Roskilde: Roskilde University , 24–50.
- Hottung, A., Tierney, K., 2020. Neural large neighborhood search for the capacitated vehicle routing problem, in: *European Conference on Artificial Intelligence*, pp. 443–450. doi:10.3233/FAIA200124.
- Hudson, B., Li, Q., Malencia, M., Prorok, A., 2022. Graph neural network guided local search for the traveling salesperson problem, in: *ICLR 2022 - 10th International Conference on Learning Representations*.
- Jan, Z., Ahamed, F., Mayer, W., Patel, N., Grossmann, G., Stumptner, M., Kuusk, A., 2023. Artificial intelligence for industry 4.0: Systematic review of applications, challenges, and opportunities. *Expert Systems with Applications* 216, 119456. URL: <https://www.sciencedirect.com/science/article/pii/S0957417422024757>, doi:https://doi.org/10.1016/j.eswa.2022.119456.
- Kalatzantonakis, P., Sifaleras, A., Samaras, N., 2023. A reinforcement learning-variable neighborhood search method for the capacitated vehicle routing problem. *Expert Systems with Applications* 213, 118812. URL: <https://www.sciencedirect.com/science/article/pii/S0957417422018309>, doi:10.1016/j.eswa.2022.118812.
- Kim, M., Park, J., Kim, J., 2021. Learning collaborative policies to solve np-hard routing problems, in: *Advances in Neural Information Processing Systems*, pp. 10418–10430.
- Kim, M., Park, J., Park, J., 2022. Sym-nco: Leveraging symmetry for neural combinatorial optimization, in: *Advances in Neural Information Processing Systems*.
- Kingma, D.P., Ba, J., 2015. Adam: A method for stochastic optimization, in: *3rd International Conference on Learning Representations, ICLR 2015 - Conference Track Proceedings*.
- Kool, W., van Hoof, H., Welling, M., 2019. Attention, learn to solve routing problems!, in: *7th International Conference on Learning Representations, ICLR 2019*.
- Kwon, Y.D., Choo, J., Kim, B., Yoon, I., Gwon, Y., Min, S., 2020. Pomo: Policy optimization with multiple optima for reinforcement learning, in: *Advances in Neural Information Processing Systems*.

- Kwon, Y.D., Choo, J., Yoon, I., Park, M., Park, D., Gwon, Y., 2021. Matrix encoding networks for neural combinatorial optimization, in: *Advances in Neural Information Processing Systems*, pp. 5138–5149.
- Lei, K., Guo, P., Wang, Y., Wu, X., Zhao, W., 2022. Solve routing problems with a residual edge-graph attention neural network. *Neurocomputing* 508, 79–98. doi:[10.1016/j.neucom.2022.08.005](https://doi.org/10.1016/j.neucom.2022.08.005).
- Li, C., Zheng, P., Yin, Y., Wang, B., Wang, L., 2023. Deep reinforcement learning in smart manufacturing: A review and prospects. *CIRP Journal of Manufacturing Science and Technology* 40, 75–101. doi:[10.1016/J.CIRPJ.2022.11.003](https://doi.org/10.1016/J.CIRPJ.2022.11.003).
- Li, J., Dai, B.T., Niu, Y., Xiao, J., Wu, Y., 2024. Multi-type attention for solving multi-depot vehicle routing problems. *IEEE Transactions on Intelligent Transportation Systems* doi:[10.1109/TITS.2024.3413077](https://doi.org/10.1109/TITS.2024.3413077).
- Li, S., Yan, Z., Wu, C., 2021. Learning to delegate for large-scale vehicle routing, in: *Advances in Neural Information Processing Systems*, pp. 26198–26211.
- Li, Y., Chu, F., Feng, C., Chu, C., Zhou, M.C., 2019. Integrated production inventory routing planning for intelligent food logistics systems. *IEEE Transactions on Intelligent Transportation Systems* 20, 867–878. doi:[10.1109/TITS.2018.2835145](https://doi.org/10.1109/TITS.2018.2835145).
- Lin, Z., Wu, Y., Zhou, B., Cao, Z., Song, W., Zhang, Y., Jayavelu, S., 2024. Cross-problem learning for solving vehicle routing problems, in: *IJCAI International Joint Conference on Artificial Intelligence*, pp. 6958–6966.
- Liu, F., Lin, X., Wang, Z., Zhang, Q., Xialiang, T., Yuan, M., 2024. Multi-task learning for routing problem with cross-problem zero-shot generalization, in: *Proceedings of the ACM SIGKDD International Conference on Knowledge Discovery and Data Mining*, pp. 1898–1908. doi:[10.1145/3637528.3672040](https://doi.org/10.1145/3637528.3672040).
- Luo, F., Lin, X., Liu, F., Zhang, Q., Wang, Z., 2023. Neural combinatorial optimization with heavy decoder: Toward large scale generalization, in: *Advances in Neural Information Processing Systems*.
- Ma, Y., Cao, Z., Chee, Y.M., 2023. Learning to search feasible and infeasible regions of routing problems with flexible neural k-opt, in: *Advances in Neural Information Processing Systems*.
- Ma, Y., Li, J., Cao, Z., Song, W., Zhang, L., Chen, Z., Tang, J., 2021. Learning to iteratively solve routing problems with dual-aspect collaborative transformer, in: *Advances in Neural Information Processing Systems*, pp. 11096–11107.
- Manchanda, S., Michel, S., Drakulic, D., Andreoli, J.M., 2023. On the generalization of neural combinatorial optimization heuristics, in: Amini, M.R., Canu, S., Fischer, A., Guns, T., Novak, P.K., Tsoumakas, G. (Eds.), *Machine Learning and Knowledge Discovery in Databases*, Springer Nature Switzerland. pp. 426–442.
- Marinakis, Y., Marinaki, M., 2010. A hybrid genetic – particle swarm optimization algorithm for the vehicle routing problem. *Expert Systems with Applications* 37, 1446–1455. URL: <https://www.sciencedirect.com/science/article/pii/S0957417409006460>, doi:[10.1016/j.eswa.2009.06.085](https://doi.org/10.1016/j.eswa.2009.06.085).
- Mazyavkina, N., Sviridov, S., Ivanov, S., Burnaev, E., 2021. Reinforcement learning for combinatorial optimization: A survey. doi:[10.1016/j.cor.2021.105400](https://doi.org/10.1016/j.cor.2021.105400).
- Nagata, Y., Kobayashi, S., 2010. A memetic algorithm for the pickup and delivery problem with time windows using selective route exchange crossover, in: Carlos, Joanna, K., Robert, R.G.S., Cotta (Eds.), *Parallel Problem Solving from Nature, PPSN XI*, Springer Berlin Heidelberg. pp. 536–545.
- Nazari, M., Oroojlooy, A., Takáč, M., Snyder, L.V., 2018. Reinforcement learning for solving the vehicle routing problem, in: *Advances in Neural Information Processing Systems*, pp. 9839–9849.
- Pan, S.J., Yang, Q., 2010. A survey on transfer learning. *IEEE Transactions on Knowledge and Data Engineering* 22, 1345–1359. doi:[10.1109/TKDE.2009.191](https://doi.org/10.1109/TKDE.2009.191).
- Paszke, A., Gross, S., Chintala, S., Chanan, G., Yang, E., DeVito, Z., Lin, Z., Desmaison, A., Antiga, L., Lerer, A., 2017. Automatic differentiation in pytorch.
- Pessoa, A., Sadykov, R., Uchoa, E., Vanderbeck, F., 2020. A generic exact solver for vehicle routing and related problems. *Mathematical Programming* 183, 483–523. doi:[10.1007/s10107-020-01523-z](https://doi.org/10.1007/s10107-020-01523-z).
- Pirnay, J., Grimm, D.G., 2024. Self-improvement for neural combinatorial optimization: Sample without replacement, but improvement. *Transactions on Machine Learning Research*.
- Reinelt, G., 1991. TspLib—a traveling salesman problem library. *ORSA Journal on Computing* 3, 376–384. doi:[10.1287/ijoc.3.4.376](https://doi.org/10.1287/ijoc.3.4.376).
- Renaud, J., Laporte, G., Boctor, F.F., 1996. A tabu search heuristic for the multi-depot vehicle routing problem. *Computers & Operations Research* 23, 229–235. URL: <https://www.sciencedirect.com/science/article/pii/S030505489500026P>, doi:[10.1016/0305-0548\(95\)00026-P](https://doi.org/10.1016/0305-0548(95)00026-P).
- Roberto, P., Costa, O.D., Rhuggenaath, J., Zhang, Y., Akcay, A., 2020. Learning 2-opt heuristics for the traveling salesman problem via deep reinforcement learning, in: *Proceedings of Machine Learning Research*, pp. 465–480.
- Sadati, M.E.H., Çatay, B., Aksen, D., 2021. An efficient variable neighborhood search with tabu shaking for a class of multi-depot vehicle routing problems. *Computers & Operations Research* 133, 105269. URL: <https://www.sciencedirect.com/science/article/pii/S0305054821000617>, doi:[10.1016/j.cor.2021.105269](https://doi.org/10.1016/j.cor.2021.105269).
- Silva, M.A.L., de Souza, S.R., Souza, M.J.F., Bazzan, A.L.C., 2019. A reinforcement learning-based multi-agent framework applied for solving routing and scheduling problems. *Expert Systems with Applications* 131, 148–171. URL: <https://www.sciencedirect.com/science/article/pii/S0957417419302866>, doi:[10.1016/j.eswa.2019.04.056](https://doi.org/10.1016/j.eswa.2019.04.056).
- Solomon, M.M., 1987. Algorithms for the vehicle routing and scheduling problems with time window constraints. *Oper. Res.* 35, 254–265.
- Sutton, R.S., Barto, A.G., 1998. Reinforcement learning: An introduction. *IEEE Transactions on Neural Networks* 9, 1054. doi:[10.1109/TNN.1998.712192](https://doi.org/10.1109/TNN.1998.712192).
- Uchoa, E., Pecin, D., Pessoa, A., Poggi, M., Vidal, T., Subramanian, A., 2017. New benchmark instances for the capacitated vehicle routing problem. *European Journal of Operational Research* 257, 845–858. doi:[10.1016/j.ejor.2016.08.012](https://doi.org/10.1016/j.ejor.2016.08.012).
- Vaswani, A., Shazeer, N.M., Parmar, N., Uszkoreit, J., Jones, L., Gomez, A.N., Kaiser, L., Polosukhin, I., 2017. Attention is all you need, in: *Advances in Neural Information Processing Systems*, pp. 5999–6009.



- Veličković, P., Cucurull, G., Casanova, A., Romero, A., Liò, P., Bengio, Y., 2018. Graph attention networks, in: 6th International Conference on Learning Representations, ICLR 2018 - Conference Track Proceedings.
- Vidal, T., 2022. Hybrid genetic search for the cvrp: Open-source implementation and swap\* neighborhood. *Computers and Operations Research* 140. doi:[10.1016/j.cor.2021.105643](https://doi.org/10.1016/j.cor.2021.105643).
- Vinyals, O., Fortunato, M., Jaitly, N., 2015. Pointer networks, in: *Advances in Neural Information Processing Systems*, pp. 2692–2700.
- Wang, Z., Sheu, J.B., 2019. Vehicle routing problem with drones. *Transportation Research Part B: Methodological* 122, 350–364. URL: <https://www.sciencedirect.com/science/article/pii/S0191261518307884>, doi:[10.1016/j.trb.2019.03.005](https://doi.org/10.1016/j.trb.2019.03.005).
- Williams, R.J., 1992. Simple statistical gradient-following algorithms for connectionist reinforcement learning. *Machine Learning* 8, 229–256. URL: <https://doi.org/10.1007/BF00992696>, doi:[10.1007/BF00992696](https://doi.org/10.1007/BF00992696).
- Wouda, N.A., Lan, L., Kool, W., 2024. Pyvrp: A high-performance vrp solver package. *INFORMS Journal on Computing* 36, 943–955. doi:[10.1287/ijoc.2023.0055](https://doi.org/10.1287/ijoc.2023.0055).
- Wu, Y., Song, W., Cao, Z., Zhang, J., Lim, A., 2022. Learning improvement heuristics for solving routing problems. *IEEE Transactions on Neural Networks and Learning Systems* 33, 5057–5069. doi:[10.1109/TNNLS.2021.3068828](https://doi.org/10.1109/TNNLS.2021.3068828).
- Wu, Y., Zhou, J., Xia, Y., Zhang, X., Cao, Z., Zhang, J., 2023. Neural airport ground handling. *IEEE Transactions on Intelligent Transportation Systems* 24, 15652–15666. doi:[10.1109/TITS.2023.3253552](https://doi.org/10.1109/TITS.2023.3253552).
- Xin, L., Song, W., Cao, Z., Zhang, J., 2020. Multi-decoder attention model with embedding glimpse for solving vehicle routing problems, in: *AAAI Conference on Artificial Intelligence*.
- Xin, L., Song, W., Cao, Z., Zhang, J., 2021. Neurolkh: Combining deep learning model with lin-kernighan-helsgaun heuristic for solving the traveling salesman problem, in: *Advances in Neural Information Processing Systems*, pp. 7472–7483.
- Xu, L., Brintrup, A., Baryannis, G., Ivanov, D., 2024. Data-driven logistics and supply chain competition incom 2024. URL: <https://www.incom2024.org/data-challenge/>.
- Yuan, X.T., Liu, X., Yan, S., 2012. Visual classification with multitask joint sparse representation. *IEEE Transactions on Image Processing* 21, 4349–4360.
- Zhang, H., Ge, H., Yang, J., Tong, Y., 2022. Review of vehicle routing problems: Models, classification and solving algorithms. *Archives of Computational Methods in Engineering* 29, 195–221. URL: <https://doi.org/10.1007/s11831-021-09574-x>, doi:[10.1007/s11831-021-09574-x](https://doi.org/10.1007/s11831-021-09574-x).
- Zhang, Y., Yang, Q., 2022. A survey on multi-task learning. *IEEE Transactions on Knowledge and Data Engineering* 34, 5586–5609. doi:[10.1109/TKDE.2021.3070203](https://doi.org/10.1109/TKDE.2021.3070203).
- Zhou, J., Cao, Z., Wu, Y., Song, W., Ma, Y., Zhang, J., Xu, C., 2024a. Mvmoe: Multi-task vehicle routing solver with mixture-of-experts. *Proceedings of Machine Learning Research*, 61804–61824.
- Zhou, J., Wu, Y., Cao, Z., Song, W., Zhang, J., Shen, Z., 2024b. Collaboration! towards robust neural methods for routing problems, in: *Advances in Neural Information Processing Systems*, pp. 121731–121764.
- Zhou, J., Wu, Y., Song, W., Cao, Z., Zhang, J., 2023. Towards omni-generalizable neural methods for vehicle routing problems, in: *Proceedings of Machine Learning Research*, pp. 42769–42789.

## Appendix A. Hyper-parameters sensitivity

In this appendix, we analyze the sensitivities of various hyper-parameters in our approach. Specifically, we examine the impact of the number of encoder layers  $L$ , the number of heads in the decoder  $H$ , the hidden dimension  $h_x$  and the hidden edge dimension  $h_e$ .

First, we assessed the model’s sensitivity to the number of encoder layers by testing values of  $L = 3, 4, 5, 6$ . Fig. A.1 presents the average cost during pre-training for each value over 100 episodes. Interestingly, the model’s performance degraded when using 6 encoder layers, yielding results comparable to those obtained with 3 layers. In contrast, models with 4 and 5 encoder layers performed better, with the 5-layer configuration showing a slight edge over the 4-layer model.

For the other hyper-parameters, we explored four different combinations, as shown in Fig. A.2. The best-performing configuration used a hidden dimension of  $h_x = 256$ , a hidden edge dimension of  $h_e = 32$  and  $H = 16$  heads in the decoder.

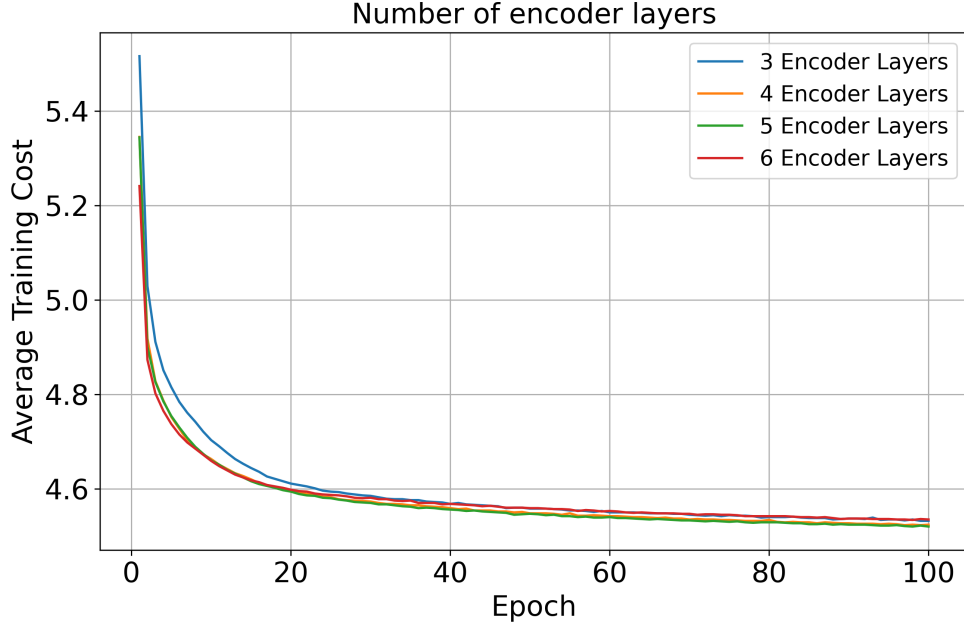


Figure A.1: Sensitivity analysis of the number of encoder layers  $L$ .

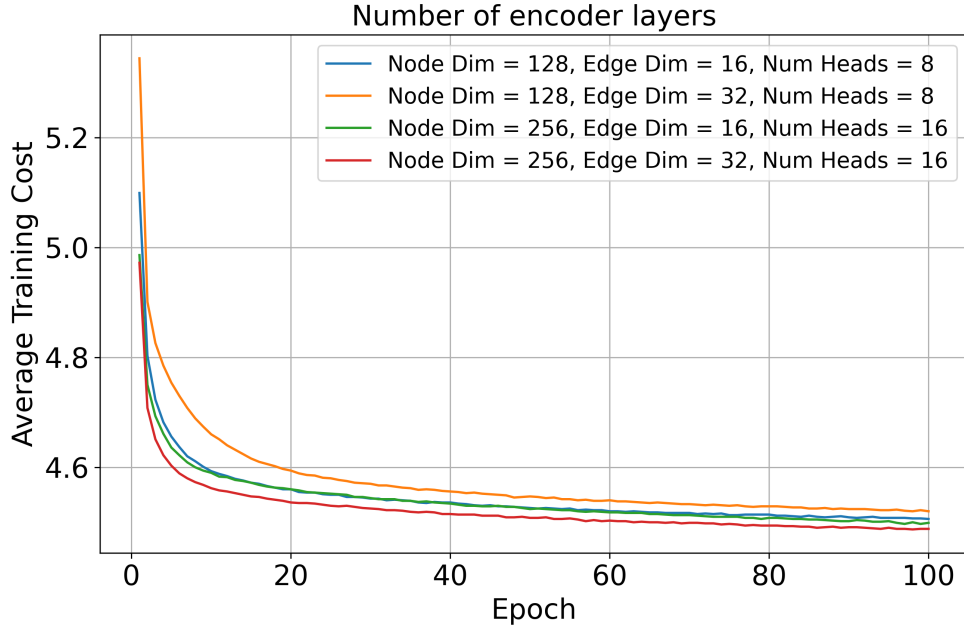


Figure A.2: Sensitivity analysis of the hidden dimension  $h_x$ , hidden edge dimension  $h_e$  and number of heads  $H$ .

## Appendix B. Instance generation

To generate the random training and testing instances for all VRP variants (including  $n = 20$ ,  $n = 50$  and  $n = 100$ ), we uniformly sample node coordinates within a  $[0, 1] \times [0, 1]$  Euclidean space. Customer demands are randomly sampled from 1, ..., 9 and then normalized with respect to vehicle capacity, which is set to 50. Additional data is generated depending on the VRP variant considered. We follow similar settings as other research, which are described next. 1) VRPB: We randomly select 20% of the customers as backhauls, following Liu et al. (2024). Our paper considers mixed backhauls, meaning linehaul and backhaul customers can be visited without a strict precedence order. However, the vehicle’s capacity constraints must always be respected. For this reason, every route must start with a linehaul customer. 2) VRPL: We set a length limit of 3 for all routes, again following Liu et al. (2024). 3) VRPTW: For the VRPTW, we follow the same procedure as Solomon (1987), Li et al. (2021) and Zhou et al. (2024a) for generating the service times and time windows.

## Appendix C. Generalization on INCOM2024 benchmark instances

We present results on additional MDVRP benchmark instances on Table C.1. We evaluated TuneNSearch performance using instances from INCOM 2024 data-drive logistics challenge dataset (Xu et al., 2024). This dataset was introduced by the Supply Chain AI Lab (SCAIL) of the University of Cambridge at the INCOM 2024 Conference for a logistics challenge, which can be downloaded via the link <sup>1</sup>. It includes 100 instances with problem sizes ranging from 100 to 1000 nodes. To benchmark this dataset, we executed PyVRP using the same time limit as Vidal (2022) and Wouda et al. (2024). We used the same experimental setup from Section 5.2. As with Cordeau’s dataset, TuneNSearch consistently outperformed the MD-MTA and POMO models. These results further demonstrate the strong generalization capabilities of TuneNSearch, even when applied to problems of larger scale with different distributions.

Table C.1: Generalization on INCOM 2024 benchmark instances.

Instance	Depots	Customers	PyVRP	Ours		MD-MTA		POMO	
				Obj.	Gap	Obj.	Gap	Obj.	Gap
scail01	4	100	13099	<b>13315</b>	<b>1.649</b> %	13831	5.588 %	13855	5.771 %
scail02	3	105	9590	<b>9727</b>	<b>1.429</b> %	10023	4.515 %	10153	5.871 %
scail03	3	110	11772	<b>11929</b>	<b>1.334</b> %	12273	4.256 %	12257	4.120 %
scail04	4	115	10600	<b>10714</b>	<b>1.075</b> %	11182	5.491 %	10987	3.651 %
scail05	2	119	16374	<b>16739</b>	<b>2.229</b> %	17196	5.020 %	16965	3.609 %
scail06	4	123	11159	<b>11329</b>	<b>1.523</b> %	11934	6.945 %	11842	6.121 %
scail07	3	127	8544	<b>8690</b>	<b>1.709</b> %	10160	18.914 %	9573	12.044 %
scail08	2	132	11846	<b>12011</b>	<b>1.393</b> %	12502	5.538 %	12229	3.233 %
scail09	4	137	8811	<b>9091</b>	<b>3.178</b> %	10223	16.025 %	9840	11.679 %
scail10	2	142	17173	<b>17196</b>	<b>0.134</b> %	18101	5.404 %	18088	5.328 %
scail11	3	147	10626	<b>10934</b>	<b>2.899</b> %	12010	13.025 %	11604	9.204 %
scail12	4	151	13504	<b>13800</b>	<b>2.192</b> %	14498	7.361 %	14831	9.827 %
scail13	3	156	13312	<b>13578</b>	<b>1.998</b> %	14576	9.495 %	15522	16.602 %
scail14	2	161	9785	<b>9984</b>	<b>2.034</b> %	10735	9.709 %	10756	9.923 %
scail15	4	165	16071	<b>16690</b>	<b>3.852</b> %	17917	11.486 %	17631	9.707 %
scail16	3	170	15011	<b>15205</b>	<b>1.292</b> %	16149	7.581 %	16255	8.287 %
scail17	3	175	13712	<b>13937</b>	<b>1.641</b> %	14925	8.846 %	14616	6.593 %
scail18	2	180	15144	<b>15384</b>	<b>1.585</b> %	16469	8.749 %	16514	9.046 %
scail19	2	184	20116	<b>20710</b>	<b>2.953</b> %	21518	6.970 %	21615	7.452 %

<sup>1</sup><https://www.ifm.eng.cam.ac.uk/research/supply-chain-ai-lab/data-competition/>

scail20	2	189	24494	<b>25012</b>	<b>2.115</b> %	26196	6.949 %	26504	8.206 %
scail21	2	194	14079	<b>14415</b>	<b>2.387</b> %	15592	10.746 %	16350	16.130 %
scail22	4	198	35731	<b>35750</b>	<b>0.053</b> %	38619	8.083 %	38663	8.206 %
scail23	4	202	13357	<b>13857</b>	<b>3.743</b> %	14996	12.271 %	14753	10.451 %
scail24	2	206	37615	<b>38417</b>	<b>2.132</b> %	40864	8.637 %	41506	10.344 %
scail25	3	210	19067	<b>19735</b>	<b>3.503</b> %	20680	8.460 %	20888	9.551 %
scail26	3	214	12428	<b>12749</b>	<b>2.583</b> %	13840	11.361 %	14154	13.888 %
scail27	4	219	21051	<b>21748</b>	<b>3.311</b> %	23309	10.726 %	23643	12.313 %
scail28	3	224	13236	<b>13796</b>	<b>4.231</b> %	14574	10.109 %	14860	12.270 %
scail29	3	228	29825	<b>30508</b>	<b>2.290</b> %	32370	8.533 %	33266	11.537 %
scail30	3	233	33578	<b>34537</b>	<b>2.856</b> %	37066	10.388 %	36983	10.141 %
scail31	2	238	31881	<b>32297</b>	<b>1.305</b> %	35048	9.933 %	34649	8.682 %
scail32	3	242	11293	<b>11703</b>	<b>3.631</b> %	13337	18.100 %	13974	23.740 %
scail33	2	247	27116	<b>27907</b>	<b>2.917</b> %	29881	10.197 %	31910	17.680 %
scail34	4	252	20586	<b>20924</b>	<b>1.642</b> %	22623	9.895 %	22777	10.643 %
scail35	2	257	43163	<b>44465</b>	<b>3.016</b> %	47174	9.293 %	47704	10.521 %
scail36	2	262	41070	<b>42635</b>	<b>3.811</b> %	44628	8.663 %	45390	10.519 %
scail37	3	266	17771	<b>17959</b>	<b>1.058</b> %	19691	10.804 %	20176	13.533 %
scail38	4	270	20579	<b>21406</b>	<b>4.019</b> %	23223	12.848 %	23172	12.600 %
scail39	3	275	27075	<b>27390</b>	<b>1.163</b> %	29875	10.342 %	30323	11.996 %
scail40	2	279	28127	<b>29162</b>	<b>3.680</b> %	31097	10.559 %	31583	12.287 %
scail41	3	284	26304	<b>27263</b>	<b>3.646</b> %	30426	15.671 %	30467	15.826 %
scail42	3	288	17468	<b>18343</b>	<b>5.009</b> %	19965	14.295 %	20089	15.005 %
scail43	2	293	27788	<b>28379</b>	<b>2.127</b> %	30663	10.346 %	32270	16.129 %
scail44	3	297	25846	<b>26859</b>	<b>3.919</b> %	29160	12.822 %	29033	12.331 %
scail45	2	302	27694	<b>28639</b>	<b>3.412</b> %	31177	12.577 %	31445	13.544 %
scail46	3	309	35469	<b>36498</b>	<b>2.901</b> %	39411	11.114 %	40518	14.235 %
scail47	2	315	16346	<b>17035</b>	<b>4.215</b> %	18443	12.829 %	19669	20.329 %
scail48	2	323	24758	<b>25840</b>	<b>4.370</b> %	28175	13.802 %	27146	9.645 %
scail49	3	330	22161	<b>22507</b>	<b>1.561</b> %	25948	17.089 %	28425	28.266 %
scail50	3	337	13857	<b>14644</b>	<b>5.679</b> %	16729	20.726 %	17235	24.378 %
scail51	3	345	24642	<b>25799</b>	<b>4.695</b> %	28033	13.761 %	28790	16.833 %
scail52	3	352	17769	<b>18774</b>	<b>5.656</b> %	20833	17.243 %	21473	20.845 %
scail53	3	358	25662	<b>26526</b>	<b>3.367</b> %	28809	12.263 %	29691	15.700 %
scail54	2	364	32397	<b>33196</b>	<b>2.466</b> %	36680	13.220 %	37105	14.532 %
scail55	3	370	21246	<b>22448</b>	<b>5.658</b> %	24650	16.022 %	25102	18.149 %
scail56	3	377	18647	<b>19261</b>	<b>3.293</b> %	21757	16.678 %	22436	20.320 %
scail57	2	385	38457	<b>40063</b>	<b>4.176</b> %	43683	13.589 %	44039	14.515 %
scail58	3	393	17678	<b>18773</b>	<b>6.194</b> %	21156	19.674 %	22078	24.890 %
scail59	3	401	86457	<b>87953</b>	<b>1.730</b> %	96866	12.039 %	103530	19.747 %
scail60	4	413	30626	<b>32282</b>	<b>5.407</b> %	35540	16.045 %	36085	17.825 %
scail61	3	424	33534	<b>34993</b>	<b>4.351</b> %	39134	16.699 %	39060	16.479 %
scail62	3	438	29444	<b>30866</b>	<b>4.830</b> %	33676	14.373 %	35219	19.613 %
scail63	2	452	33495	<b>33554</b>	<b>0.176</b> %	37117	10.813 %	38676	15.468 %
scail64	3	466	31934	<b>33371</b>	<b>4.500</b> %	37029	15.955 %	37896	18.670 %
scail65	3	480	17811	<b>18780</b>	<b>5.440</b> %	21959	23.289 %	23293	30.779 %
scail66	3	493	68424	<b>69353</b>	<b>1.358</b> %	75055	9.691 %	79200	15.749 %
scail67	4	506	41279	<b>42795</b>	<b>3.673</b> %	47398	14.823 %	49355	19.564 %
scail68	4	516	30812	<b>32249</b>	<b>4.664</b> %	36866	19.648 %	36288	17.772 %
scail69	3	526	23097	<b>23984</b>	<b>3.840</b> %	34706	50.262 %	37294	61.467 %
scail70	2	535	30467	<b>31229</b>	<b>2.501</b> %	36158	18.679 %	39932	31.066 %

scail71	3	548	44511	<b>45454</b>	<b>2.119</b> %	51096	14.794 %	52273	17.438 %
scail72	2	560	58858	<b>60956</b>	<b>3.565</b> %	67969	15.480 %	69224	17.612 %
scail73	4	573	26192	<b>27230</b>	<b>3.963</b> %	31052	18.555 %	34598	32.094 %
scail74	2	587	63596	<b>66061</b>	<b>3.876</b> %	72128	13.416 %	73651	15.811 %
scail75	2	597	55622	<b>57610</b>	<b>3.574</b> %	66019	18.692 %	67546	21.438 %
scail76	3	609	41069	<b>42303</b>	<b>3.005</b> %	47966	16.794 %	53417	30.066 %
scail77	3	625	102859	<b>104795</b>	<b>1.882</b> %	117132	13.876 %	119924	16.591 %
scail78	3	641	43495	<b>45432</b>	<b>4.453</b> %	50906	17.039 %	53488	22.975 %
scail79	4	656	42247	<b>43888</b>	<b>3.884</b> %	50346	19.171 %	53284	26.125 %
scail80	4	672	46051	<b>47185</b>	<b>2.462</b> %	53573	16.334 %	58291	26.579 %
scail81	3	687	21921	<b>23790</b>	<b>8.526</b> %	28812	31.436 %	30874	40.842 %
scail82	4	702	49390	<b>50789</b>	<b>2.833</b> %	57085	15.580 %	66046	33.723 %
scail83	3	717	49456	<b>51915</b>	<b>4.972</b> %	58367	18.018 %	62634	26.646 %
scail84	4	733	18124	<b>19757</b>	<b>9.010</b> %	24508	35.224 %	28168	55.418 %
scail85	2	748	51616	<b>54245</b>	<b>5.093</b> %	61848	19.823 %	62601	21.282 %
scail86	3	763	33514	<b>35387</b>	<b>5.589</b> %	40891	22.012 %	43619	30.152 %
scail87	3	779	31036	<b>33101</b>	<b>6.654</b> %	39041	25.793 %	45531	46.704 %
scail88	3	795	41243	<b>43654</b>	<b>5.846</b> %	53080	28.701 %	54856	33.007 %
scail89	4	811	22990	<b>24662</b>	<b>7.273</b> %	31070	35.146 %	34960	52.066 %
scail90	3	826	68092	<b>69168</b>	<b>1.580</b> %	77239	13.433 %	82490	21.145 %
scail91	4	841	22835	<b>24227</b>	<b>6.096</b> %	31508	37.981 %	38902	70.361 %
scail92	4	856	58744	<b>59867</b>	<b>1.912</b> %	71191	21.188 %	74127	26.187 %
scail93	4	871	49517	<b>50694</b>	<b>2.377</b> %	59129	19.411 %	67289	35.891 %
scail94	2	887	76542	<b>78704</b>	<b>2.825</b> %	90743	18.553 %	96481	26.050 %
scail95	2	903	107324	<b>108076</b>	<b>0.701</b> %	119771	11.596 %	135159	25.935 %
scail96	2	922	82326	<b>82908</b>	<b>0.707</b> %	95933	16.528 %	100659	22.269 %
scail97	2	942	103103	<b>107592</b>	<b>4.354</b> %	118724	15.151 %	122495	18.808 %
scail98	4	962	37379	<b>40669</b>	<b>8.802</b> %	48431	29.567 %	52647	40.846 %
scail99	4	982	37400	<b>39561</b>	<b>5.778</b> %	47544	27.123 %	58895	57.473 %
scail100	4	1002	29043	<b>30601</b>	<b>5.364</b> %	39199	34.969 %	45220	55.700 %
Avg. Gap				<b>3.354</b> %		15.052 %		19.702 %	